
**“ROLE OF HIGH RESOLUTION COMPUTED TOMOGRAPHY THORAX IN
ASSESSMENT OF VARIOUS IMAGING PATTERNS IN CHRONIC
OBSTRUCTIVE PULMONARY DISEASE-A ONE YEAR CROSS SECTIONAL
STUDY IN A TERTIARY CARE HOSPITAL”**

**BY
REG. NO. BS0122013**

Dissertation

**Submitted to the
KLE Academy of Higher Education and Research, Belagavi, Karnataka
In partial fulfilment
of the requirements for the degree of**

**M.D.
IN
RADIO-DIAGNOSIS
DEPARTMENT OF RADIO-DIAGNOSIS, J. N. MEDICAL COLLEGE,
BELAGAVI - 590010. KARNATAKA**

SEPTEMBER / OCTOBER 2025

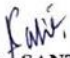
**KLE ACADEMY OF HIGHER EDUCATION AND RESEARCH
BELAGAVI, KARNATAKA**

KLE ACADEMY OF HIGHER EDUCATION AND RESEARCH,
BELAGAVI

**Endorsement by the HOD/ Principal/
Head of the Institution**


This is to certify that the dissertation entitled "ROLE OF HIGH RESOLUTION COMPUTED TOMOGRAPHY THORAX IN ASSESSMENT OF VARIOUS IMAGING PATTERNS IN CHRONIC OBSTRUCTIVE PULMONARY DISEASE-A ONE YEAR CROSS SECTIONAL STUDY IN A TERTIARY CARE HOSPITAL." is a bonafide research work done by

REG NO: BS0122013.


Dr. SANTOSH D. PATIL
MD (RADIO DIAGNOSIS) & HOD
Professor and Head
Department of Radiodiagnosis,
J. N. Medical College,
Nehru Nagar, Belagavi - 10

Date : 24/03/2025
Place : Belagavi




Dr. (Mrs.) N.S. MAHANTSHETTI
MD (PAEDIATRICS)
Principal,
J. N. Medical College,
Nehru Nagar, Belagavi - 10

Date : 25/03/25
Place : Belagavi
PRINCIPAL
Jawaharlal Nehru Medical College
BELAGAVI

© KLE Academy of higher Education and Research
Belagavi, Karnataka

UNDERTAKING

I, Reg. No. BS0122013, hereby declare that the information and the data mentioned in my dissertation entitled “**ROLE OF HIGH RESOLUTION COMPUTED TOMOGRAPHY THORAX IN ASSESSMENT OF VARIOUS IMAGING PATTERNS IN CHRONIC OBSTRUCTIVE PULMONARY DISEASE-A ONE YEAR CROSS SECTIONAL STUDY IN A TERTIARY CARE HOSPITAL**” belongs to me and is original. I am aware of the definition of plagiarism as detailed below:

- ❖ An act or instance of using or closely imitating the language and thoughts of another author without authorization and the representation of that author’s work as one’s own, as by not crediting the original author.
- ❖ A piece of writing or other work reflecting such unauthorized use or imitation.
- ❖ The deliberate or reckless representation of another’s words, thoughts or ideas as one’s own without a
- ❖ attribution in connection with submission of academic work, whether graded or otherwise.



I hereby declare that the dissertation prepared by me is original one and does not involve plagiarism anywhere. In case at a later stage, it is found that I have indulged in plagiarism, then I am solely responsible for the same and the institution is at liberty to take any disciplinary action against me including cancellation of dissertation or any other penalties imposed by the University.

Date: 25/03/25

Place: Belagavi



(REG BS0122013)


PLAGIARISM ACCEPTANCE LETTER


	JAWAHARLAL NEHRU MEDICAL COLLEGE (A constituent unit of KLE Academy of Higher Education & Research Deemed-to-be-University) (Recognized by National Medical Commission, New Delhi)	
Accredited 'A+' Grade by NAAC (3 rd Cycle)		Placed in Category 'A' by MoE (GoI)
Nehru Nagar, Belagavi- 590 010, Karnataka, INDIA		
☎ 0831 - 2471350	☎ 0831 - 2470759	🌐 www.jnmc.edu
		✉ incipal@jnmc.edu
Ref No: MDC/PG/		Date: 17-03-2025

"ACCEPTANCE LETTER"

The softcopy of thesis entitled: "ROLE OF HIGH RESOLUTION COMPUTED TOMOGRAPHY THORAX IN ASSESSMENT OF VARIOUS IMAGING PATTERNS IN CHRONIC OBSTRUCTIVE PULMONARY DISEASE-A ONE YEAR CROSS SECTIONAL STUDY IN A TERTIARY CARE HOSPITAL" has been submitted for anti-plagiarism check through Turnitin software. The scan has been carried out and the scanned output reveals a match percentage of 06% which is within the acceptable limits of 10% as per the guidelines given by UGC.





Guide.




Dr. (Mrs.) N.S. Mahantashetti.
Chairperson-Antiplagiarism Committee &
Principal,
J. N. Medical College, Belagavi.

To,
Reg. No. BS0122013
Postgraduate Student,
2022-23 Batch,
Department of Radio-Diagnosis
J. N. Medical College, Belagavi.

ETHICAL CLEARANCE CERTIFICATE

	K.L.E. ACADEMY OF HIGHER EDUCATION AND RESEARCH (Deemed - to- be- University)
	Accredited "A+" Grade by NAAC in 3 rd Cycle) Placed in Category "A" by MHRD (GoI)
JNMC INSTITUTIONAL ETHICS COMMITTEE JAWAHARLAL NEHRU MEDICAL COLLEGE, NEHRU NAGAR, BELAGAVI-590010 (KARNATAKA-INDIA)	
Website: http://www.jnmc.edu E-Mail : dome@jnmc.edu	Phone: (+ 91-(0)831 Office : 2472550 Principal: 2471701 Fax No. +91 (0)831 – 2470759
Ref No.MDC/JNMCIEC/ 201	Date: 12/05/2023
To,	
BS0122013 PG Student in Radio-Diagnosis J. N. Medical College, BELAGAVI.	
Sub: Institutional Ethical Clearance for the study.	
With reference to the above, we wish to inform you that your proposed research project titled "ROLE OF HIGH RESOLUTION COMPUTED TOMOGRAPHY THORAX IN ASSESSMENT OF VARIOUS IMAGING PATTERNS IN CHRONIC OBSTRUCTIVE PULMONARY DISEASE-A ONE YEAR CROSS SECTIONAL STUDY IN A TERTIARY CARE HOSPITAL ", is ethical and justifiable. The proposed research project has been cleared by the JNMC Institutional Ethics Committee.	
 (Dr. Smita Sonoli) Member Secretary JNMC Institutional Ethics Committee J.N.Medical College, Belagavi.	 (Dr. Harsha Hegde) Chairman, JNMC Institutional Ethics Committee J.N.Medical College, Belagavi

ABSTRACT

Background:

Chronic Obstructive Pulmonary Disease (COPD) is a progressive and heterogeneous respiratory disorder characterized by irreversible airflow limitation due to structural lung changes. Spirometry remains the gold standard for diagnosis; however, it has limitations in detecting early disease changes. High-Resolution Computed Tomography (HRCT) has emerged as an advanced imaging modality to assess early radiological abnormalities, aiding in disease characterization and management. This study aims to evaluate the role of HRCT in assessing imaging patterns in COPD patients and its potential in detecting early structural abnormalities, which may be missed by conventional spirometry.

Materials and Methods:

This hospital-based cross-sectional study was conducted over one year with a sample size of 67 COPD patients, aged 18-80 years, referred for HRCT Thorax. Patients with other respiratory illnesses were excluded. HRCT findings such as thoracic measurements, vascular attenuation, vascular distortion, mosaic attenuation, and visible small airways were recorded and analyzed using SPSS v26.0. Descriptive statistics and chi-square tests were applied, considering a p-value of <0.05 as statistically significant.

Results:

The mean age of participants was 64.65 years, with a male predominance (79.1%). Emphysematous changes were noted in 50.7%, centrilobular and combined centrilobular-paraseptal types being the most common. HRCT findings included vascular attenuation (52.2%), vascular distortion (20.9%), mosaic attenuation (41.8%), and visible small airways (34.3%). Saber Sheath Trachea (Thoracic Index <0.67) was observed in 35.8% of cases. Thoracic Cage Ratio at Carina >0.75 was noted in 11.9% of patients, while the same ratio 5 cm below the carina was slightly higher at 26.1%. Sterno-Aortic Distance >4 cm was found in 11.9% of cases. Lastly, an increased Thoracic Cross-Sectional Area/Height² (>80 cm/m²) was seen in 70.2% of patients

Conclusion:

HRCT is a valuable tool for detecting structural abnormalities in COPD, particularly in early disease stages where spirometry may be inconclusive. While this study demonstrates the utility of HRCT in COPD assessment, larger studies are needed to establish definitive associations between imaging biomarkers and disease progression.

Keywords: COPD, HRCT, emphysema, vascular attenuation, GOLD grading, small airway disease

LIST OF ABBREVIATIONS

Abbreviation	Meaning
AP	Anteroposterior
BODE	Body mass index, airflow Obstruction, Dyspnea, and Exercise capacity
CAD	Coronary artery disease
CAPTURE	Chronic obstructive pulmonary disease Assessment in Primary care To identify Undiagnosed Respiratory disease and Exacerbation risk
COPD	Chronic Obstructive Pulmonary Disease
CT	Computed Tomography
DALY	Disability-Adjusted Life Years
FEV1	Forced Expiratory Volume in One Second
FVC	Forced Vital Capacity
GINA	Global Initiative for Asthma
GOLD	Global Initiative for Chronic Obstructive Lung Disease
HIV	Human Immunodeficiency Virus
HRCT	High-Resolution Computed Tomography
HU	Hounsfeild Unit
ILD	Interstitial Lung Disease
LLA	Low-Attenuation Area
MLD	Mean Lung Density
NHLBI	National Heart, Lung, and Blood Institute
Pi	Internal Perimeter
PRM	Parametric Response Mapping
RV/TLC	Residual Volume/Total Lung Capacity
SAD	Sterno-Aortic Distance
SGRQ	St. George's Respiratory Questionnaire
TCR	Thoracic Cage Ratio
VE	Ventilation
VE/VCO2	Ventilatory Equivalent for Carbon Dioxide
WA%	Wall Area Percentage
WHO	World Health Organization
WT	Wall Thickness

TABLE OF CONTENTS

SL NO.	CONTENTS	PAGE NO.
1.	INTRODUCTION	1-3
2.	AIMS & OBJECTIVES	4
3.	REVIEW OF LITERATURE	5-23
4.	MATERIALS AND METHODS	24-28
5.	ANALYSIS AND RESULTS	29-44
6.	DISCUSSION	45-49
7.	CONCLUSION	50
8.	SUMMARY	51
9.	STRENGTHS	52
10.	LIMITATIONS	53
11.	BIBLIOGRAPHY	54-59
	ANNEXURES	
	ANNEXURE I: CONSENT FORM	60-62
	ANNEXURE II: PROFORMA	63-64
	ANNEXURE III: IMAGES	65-69
	ANNEXURE IV: KEY TO MASTER CHART	70
	ANNEXURE V: MASTER CHART	71-74

LIST OF FIGURES

Sl No.	Figure Description	Page No.
1	Figure 1: Proposed taxonomy for COPD	9
2	Figure 2: The overview of pathogenesis in COPD patients	10
3	Figure 3: Chest X-ray	14
4	Figure 4: Axial Hrct thorax with centrilobular Emphysema	15
5	Figure 5: Axial Hrct thorax with paraseptal Emphysema	16
6	Figure 6: Axial Hrct thorax with panlobular Emphysema	16
7	Figure 7: Gender distribution among the study population	31

LIST OF GRAPHS

Sl No.	Figure Description	Page No.
1	Graph 1 :Demographic characteristics of study population	30
2	Graph 2 :Bar graph demonstrating family history	33
3	Graph 3: Bar graph demonstrating the presence of smoking history	34
4	Graph 4: S Bar graph demonstrating findings of physical examination	34
5	Graph 5: Bar graph demonstrating findings of respiratory system examination	35
6	Graph 6: Bar graph demonstrating distribution according to Gold grade	36
7	Graph 7: Bar graph demonstrating the distribution of Emphysematous changes	37
8	Graph 8: Bar graph demonstrating quantitative HRCT thorax pattern for hyperinflation noted among patients	40
9	Graph 9: Bar graph demonstrating qualitative pattern for emphysema and hyperinflation seen on HRCT Thorax	41
10	Graph 10: Bar graph demonstrating association of Gold grade severity with quantitative HRCT thorax measurements	44

LIST OF TABLES

Sl No.	Table Description	Page No.
1	Table 1: Key indicators for considering a diagnosis of COPD	7
2	Table 2: Emphysema-Related CT Parameters used in various studies	23
3	Table 3: Hyperinflation, small and large airway disease-Related CT Parameters used in various studies	23
4	Table 4: Demographic characteristics of study population	30
5	Table 5: Gender distribution of study population	31
6	Table 6: Demonstrating family history, smoking history and physical examination	32
7	Table 7: Spirometry measurements of the study population	35
8	Table 8: Gold grade of study population	36
9	Table 9: Distribution of emphysematous changes	37
10	Table 10: Quantitative HRCT thorax measurement for hyperinflation	38
11	Table 11: Hyperinflation patterns of HRCT Thorax	39
12	Table 12: Qualitative patterns of emphysema and hyperinflation seen on HRCT Thorax	40
13	Table 13: Association of Gold grade severity with quantitative HRCT hyperinflation patterns	42
14	Table 14: Comparison of spirometry values with previous studies	46
15	Table 15: Comparison of emphysematous changes with previous studies	47
16	Table 16: Comparison of quantitative measurement with previous studies	47
17	Table 17: Comparison of qualitative patterns with previous studies	48

INTRODUCTION

Chronic obstructive pulmonary disease (COPD) is a prevalent, progressive, and heterogeneous group of respiratory disorders characterized by irreversible structural changes in the lung parenchyma and airways.¹ It greatly adds to the global illness burden and is one of the main causes of morbidity and death globally. Long-term exposure to harmful particles or gases is the main cause of COPD, and smoking cigarettes is the most frequent etiological component. Environmental contaminants, occupational exposures, recurring respiratory infections, genetic predispositions (such alpha-1 antitrypsin deficiency), and socioeconomic circumstances are other contributing factors.² The disease is characterized by persistent respiratory symptoms and airflow limitation due to airway remodelling, mucus hypersecretion, small airway obstruction, and emphysematous destruction of lung tissue.

Despite being a major public health issue, most often COPD is underdiagnosed, particularly in its early stages, which might delay the intervention and disease management. Conventional spirometry remains the gold standard for diagnosing COPD by assessing airflow limitation; however, it has significant limitations, particularly in detecting early disease changes. Spirometry primarily measures the forced expiratory volume in the first second (FEV₁) and the forced vital capacity (FVC), with a post-bronchodilator FEV₁/FVC ratio of less than 0.7 being the defining criterion for COPD as per the Global Initiative for Chronic Obstructive Lung Disease (GOLD) guidelines.^{3,4} However, in the early stages of COPD, spirometric readings may appear normal due to the disease's initial effects on small airways and alveolar walls, which are not adequately assessed by conventional pulmonary function tests. The Global Initiative for Chronic Obstructive Lung Disease (GOLD) grading system is a standardized method for assessing the severity of Chronic Obstructive Pulmonary Disease (COPD) based on spirometry results. It classifies COPD into four grades according to the forced expiratory volume in one second (FEV₁) percentage of predicted value. GOLD 1 (Mild) is defined as FEV₁ ≥80%, GOLD 2 (Moderate) ranges from 50% to 80%, GOLD 3 (Severe) includes 30% to 50%, and GOLD 4 (Very Severe) is FEV₁ <30%. This system helps guide treatment strategies, predict disease progression, and assess symptom burden and exacerbation risk, allowing for better disease management.

High-resolution computed tomography (HRCT) of the thorax has emerged as a valuable noninvasive diagnostic imaging tool in phenotyping, and COPD management. HRCT provides detailed visualization of lung parenchyma and airway morphology, allowing for the early identification of structural abnormalities that are not detectable by spirometry. It enables precise quantification of emphysematous changes, assessment of airway wall thickening, and detection of subtle signs of small airway disease, which are critical in understanding disease progression and heterogeneity.^{5,6} Furthermore, HRCT facilitates the differentiation of COPD phenotypes, which is crucial for personalized treatment strategies. The three primary phenotypes identified on HRCT include emphysema-predominant, chronic bronchitis-predominant, and mixed patterns, each exhibiting distinct pathophysiological mechanisms and clinical outcomes.

Since traditional spirometry frequently misses anomalies in the early stages of the illness, the main goal of this study is to use HRCT to identify and characterize the first radiological alterations in COPD. Spirometric measures may not show an increase in peripheral airway resistance right away because COPD first affects the alveolar walls and small airways. Measures of hyperinflation (such as tracheal index, sterno-aortic distance, thoracic cage ratio, and thoracic cross-sectional area), the extent of low attenuation areas indicating emphysema, and other findings like visible small airways, vascular attenuation, and vascular distortion are among the imaging markers indicative of COPD that this study intends to characterize using HRCT. Early detection of these alterations may enable prompt management, delaying the course of the illness and enhancing patient outcomes.

HRCT has several advantages over conventional imaging modalities, including its ability to provide three-dimensional, high-resolution images with superior contrast and spatial resolution. This enables the detection of subtle parenchymal changes and airway remodelling in COPD patients. For instance, HRCT can measure low-attenuation areas (LAA%), which correlate with the degree of emphysema and can be used to assess disease severity and progression. Quantitative assessment of airway dimensions, such as airway wall thickness (WA%), luminal area, and airway-to-lung ratio, further helps in phenotyping COPD. Additionally, expiratory HRCT scans have been instrumental in detecting air trapping, a hallmark of small airway disease, which is an important contributor to airflow limitation in COPD.

Various studies have validated the role of HRCT in assessment of COPD, demonstrating that HRCT-based quantification of emphysema and airway remodelling correlates well with physiological measurements, clinical symptoms, and disease outcomes. Imaging biomarkers derived from HRCT have shown promise in predicting disease exacerbations, response to treatment, and long-term prognosis.^{7,8}

Another significant application of HRCT in COPD management is its role in distinguishing COPD from other chronic respiratory conditions that present with similar clinical features. Conditions such as interstitial lung diseases (ILDs), bronchiectasis, and pulmonary vascular diseases can mimic COPD symptoms, leading to diagnostic uncertainty. HRCT provides valuable insights into the underlying pathology, aiding in accurate diagnosis and appropriate treatment planning. Additionally, HRCT can detect concomitant conditions such as lung cancer, which is more prevalent in COPD patients due to shared risk factors like smoking.^{9,10}

Despite its numerous benefits, HRCT is not routinely recommended for the diagnosis of COPD in clinical practice due to concerns regarding radiation exposure, cost, and accessibility. However, in cases where spirometry is inconclusive, symptoms are disproportionate to spirometric findings, or alternative diagnoses need to be considered, HRCT serves as a crucial adjunctive tool. The development of low-dose CT protocols and advanced image reconstruction techniques has further enhanced the feasibility of HRCT in COPD assessment by minimizing radiation exposure while maintaining image quality.

This study is particularly significant as no similar research has been conducted in this specific geographical region. The findings of this study will provide valuable insights into the spectrum of HRCT abnormalities in COPD patients within this population, contributing to a better understanding of disease patterns and phenotypic variations. By identifying key imaging markers and their correlation with clinical and spirometric parameters, this study aims to highlight the potential of HRCT as a tool for diagnosis and prognostic tool in COPD. The integration of HRCT in COPD evaluation may enable more precise disease classification, personalized treatment strategies, and improved patient management.

AIMS AND OBJECTIVES

- To identify and describe the role of HRCT Thorax in assessing different imaging patterns of COPD

REVIEW OF LITERATURE

Airflow limitation is a characteristic feature of COPD co.11,12 This impacts over 5% of the global population and is linked to significant rates of illness and death.13,14 This is ranked fourth as a leading cause of mortality in United states, with 120,000 individuals die each year.15 Due to its high prevalence and long-term nature, COPD leads to substantial resource utilization, including frequent doctor visits, recurrent hospitalizations for acute flare-ups, and ongoing treatment needs such as medication and supplemental oxygen therapy.12

Accurately diagnosing COPD is essential, as proper treatment can help alleviate symptoms (particularly dyspnea), decrease the frequency and severity of exacerbations, enhance overall health, improve exercise capacity, and extend life expectancy.16 Because current and former smokers are susceptible to various other medical conditions requiring distinct management approaches, respiratory symptoms should not be attributed to COPD without thorough evaluation and diagnosis.

Disease Burden

The occurrence, impact, and fatality rates of COPD differ between countries and among various communities within them. These variations are primarily associated with tobacco smoking prevalence. However, in some regions, such as India, air pollution from burning wood and other biomass fuels is also recognized as a significant risk factor.

The prevalence of COPD continues to rise, particularly with aging populations. It ranks as the third leading cause of death globally, contributing to approximately 2.75 million deaths annually and causing substantial morbidity.

The Disability-Adjusted Life Years (DALY) burden is estimated at 1.76 million years for the Americas and 6.74 million years for the Southeast Asian region.^{17,18} India has a significant share of global COPD-related mortality, with a rate of 102.3 deaths per 100,000 individuals and a burden of 6.74 million Disability-Adjusted Life Years (DALYs) out of the global total of 27.76 million DALYs. This has a profound impact on the country's health-related quality of life. COPD has already surpassed diseases like malaria and tuberculosis in terms of disease burden, and this gap is expected to widen further in the near future.¹⁹

Definitions

COPD should be understood in the context of other closely related common respiratory conditions (emphysema, chronic bronchitis, and chronic obstructive asthma) that represent an overlapping spectrum of airway diseases.

COPD

The Global Initiative for Chronic Obstructive Lung Disease (GOLD), a project initiated by the National Heart, Lung, and Blood Institute (NHLBI) and the World Health Organization (WHO), defines COPD as a heterogeneous lung condition characterized by chronic respiratory symptoms (dyspnea, cough, expectoration, exacerbations) due to abnormalities of the airway (bronchitis, bronchiolitis) and/or alveoli (emphysema) that cause persistent, often progressive, airflow obstruction²⁰

In practice, the diagnosis of COPD requires all of the following:

- The presence of pulmonary symptoms (dyspnea, cough, or sputum production)
- The appropriate clinical context (most notably but not exclusively tobacco exposure)
- Evidence of airflow limitation

Symptoms

- Cough
- Dyspnea
- Sputum

Risk factors

- Asthma
- Smoking
- Childhood infection
- Biomass fuel exposure
- Family history
- Prematurity

Comorbidities

- Metabolic syndrome
- Heart disease
- Sleep apnea
- Osteoporosis
- Lung cancer
- Depression

Table 1: Key indicators for considering a diagnosis of COPD

Chronic bronchitis:

Chronic bronchitis is defined by a long-lasting productive cough that persists for at least three months over two consecutive years, after ruling out other potential causes like bronchiectasis. It can develop either before or after airflow limitation sets in. While the symptom duration is somewhat arbitrarily defined, this criterion is widely accepted in research. By the ages of 35 to 40, cigarette smokers may start experiencing chronic bronchitis, along with intermittent symptom exacerbations, even in the absence of airflow obstruction.²¹⁻²³

Airflow limitation

It refers to a reduced ability to exhale efficiently, assessed by measuring the forced expiratory volume in one second (FEV1) and its ratio to the total forced expiratory volume, known as forced vital capacity (FVC). These values help determine both the presence and severity of airflow restriction. Depending on various external influences such as environmental factors, temperature fluctuations, and medication use, airflow limitation can be either fixed or variable.

Asthma is distinguished by significant variability in airflow obstruction, meaning the degree of blockage changes over time. In contrast, COPD is marked by airflow obstruction that is not fully reversible with medication, signifying a more persistent and irreversible restriction in airflow.

Asthma

The Global Initiative for Asthma (GINA) defines asthma as a chronic inflammatory condition of the airways, characterized by recurring episodes of wheezing, breathlessness, chest tightness, and coughing. These episodes are linked to widespread but variable airflow obstruction, which is often reversible either spontaneously or with treatment.

The episodic presentation of symptoms and the reversibility of airflow limitation are key clinical features that differentiate asthma from COPD. However, individuals with long-standing asthma may develop persistent airflow restriction over time. Differentiating these cases from COPD can be challenging, especially when additional COPD risk factors are present.

Classification	Description
Genetically determined COPD (COPD-G)	Alpha-1 antitrypsin deficiency (AATD) Other genetic variants with smaller effects acting in combination
COPD due to abnormal lung development (COPD-D)	Early life events, including premature birth and low birthweight, among others
Environmental COPD	
Cigarette smoking COPD (COPD-C)	<ul style="list-style-type: none"> • Exposure to tobacco smoke, including <i>in utero</i> or via passive smoking • Vaping or e-cigarette use • Cannabis
Biomass and pollution exposure COPD (COPD-P)	Exposure to household pollution, ambient air pollution, wildfire smoke, occupational hazards
COPD due to infections (COPD-I)	Childhood infections, tuberculosis-associated COPD, HIV-associated COPD
COPD & asthma (COPD-A)	Particularly childhood asthma
COPD of unknown cause (COPD-U)	

*Adapted from Celli et al. (2022) and Stolz et al. (2022)

Figure 1: Proposed taxonomy for COPD

Pathology associated with COPD

The primary pathological changes in COPD are observed in the airways, lung parenchyma, and pulmonary vasculature. The specific pattern of these changes depends on the underlying condition, such as chronic bronchitis, emphysema, alpha-1 antitrypsin deficiency, individual susceptibility, and disease severity.

CT is a valuable tool for evaluating lung parenchyma, as standard radiography is often insufficient for assessing pulmonary tissue, including the airways and vasculature.

In COPD, airway abnormalities include chronic inflammation, an increased number of goblet cells, mucus gland hyperplasia, fibrosis, and narrowing of the smaller airways. Some airways may collapse due to a loss of structural support, which occurs as a result of alveolar wall destruction, a hallmark of emphysema.²⁶

The presence of neutrophils, CD8+ T-lymphocytes, and CD68+ monocytes or macrophages in the airways can all be indicators of inflammation. ²⁸

The airflow limitations in COPD may be result of three pathological mechanisms

1. Submucosal thickening, fibrosis and narrowing of the bronchioles.
2. Disruption of alveolar attachments and loss of elastic recoil of lung
3. Small and large airways luminal obstruction by hyper-secretion of mucus and plasma exudates.

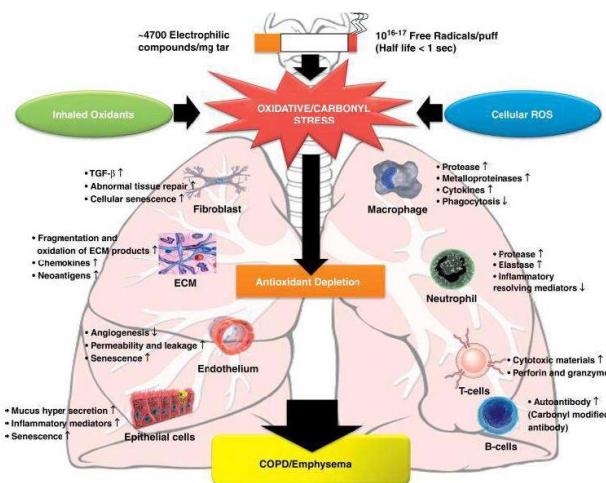


Figure 2: The overview of pathogenesis in COPD patients

The lung parenchyma involves structures located beyond the terminal bronchiole, including the respiratory bronchioles, alveolar ducts, alveolar sacs, and alveoli. Together, these components form the functional unit of gas exchange, known as the acinus.

The various subtypes of emphysema are

Proximal Acinar Emphysema – mostly affects the middle part of the acinus and is characterized by the dilatation and destruction of the respiratory bronchioles. This kind is

frequently associated with cigarette smoking, but it can also occur in those who are exposed to work-related risks, including coal miners who have pneumoconiosis.

Panacinar Emphysema – involves all of the acinus's components growing and, in some situations, being destroyed. It often coexists with alpha-1 antitrypsin deficiency and is often observed in smokers with proximal acinar emphysema.

Paraseptal Emphysema – primarily impacts the alveolar ducts and can occur alone or in conjunction with panacinar and proximal acinar emphysema. In young adults, it is frequently associated with spontaneous pneumothorax when it occurs alone.

Intimal hyperplasia and smooth muscle hypertrophy or hyperplasia are two alterations in the pulmonary vasculature that are mostly brought on by long-term hypoxia-induced vasoconstriction of the small pulmonary arteries. Several radiological imaging methods can be used to detect the distal pruning of the vasculature and the loss of the pulmonary capillary bed that occurs when these veins are destroyed.²⁹

Clinical pattern of presentation

The three cardinal symptoms of COPD are

- Dyspnea,
- Chronic Cough, and
- Sputum Production.

The most common early symptom is exertional dyspnea. Less common symptoms include wheezing and chest tightness

Approximately 62 percent of individuals with moderate to severe COPD experience fluctuations in symptoms such as shortness of breath, cough, sputum production, wheezing, and chest tightness. These variations can occur throughout the day or from week to week, with symptoms often being most severe in the morning.

COPD patients may also face weight changes, including weight gain due to reduced physical activity or weight loss, which may result from dyspnea-related eating difficulties or increased energy expenditure from labored breathing. Additionally, individuals with COPD often experience physical limitations, including restrictions in daily activities and sexual activity, as well as symptoms like coughing, syncope (fainting), depression, or anxiety. Weight loss is particularly concerning, as it is linked to advanced disease and a poorer prognosis.

Lung cancer, cardiovascular disease, bronchiectasis, skeletal muscle weakness, osteoporosis, metabolic syndrome, depression, anxiety, and cognitive impairment are among the medical diseases that frequently coexist with COPD. A family history of COPD or other chronic respiratory conditions may also be mentioned by patients.³⁰⁻³⁴

Diagnostic evaluation

The CAPTURE questionnaire (Chronic obstructive pulmonary disease Assessment in Primary care To identify Undiagnosed Respiratory disease and Exacerbation risk) is a well-validated tool that can help identify occultly symptomatic patients who would likely benefit from therapy for COPD and would therefore be candidates for diagnostic evaluation using spirometry.^{38,39}

Spirometry

Spirometry is essential for diagnosing COPD. It is typically performed before and after administering a bronchodilator to assess airflow limitation and its reversibility. A defining feature of COPD is irreversible or only partially reversible airflow limitation after bronchodilator use. If a patient does not show airflow limitation during pre-bronchodilator spirometry, they are unlikely to have COPD.

If values are abnormal, a post-bronchodilator test may be indicated. Airflow limitation that is irreversible or only partially reversible with bronchodilator is suggestive of COPD rather than asthma. Individual with pre-bronchodilator FEV1/FVC ration <0.7 that increase to ≥ 0.7 post bronchodilator has been shown to have an increased risk of future development of COPD and should be followed closely.

In the presence of a low FEV₁/FVC, the percentage of predicted FEV₁ is used to determine the severity of airflow limitation.

- GOLD 1: Mild (FEV₁ ≥80% predicted)
- GOLD 2: Moderate (50% predicted ≤FEV₁ <80% predicted)
- GOLD 3: Severe (30% predicted ≤FEV₁ <50% predicted)
- GOLD 4: Very severe (FEV₁ <30% predicted)

During spirometry, the forced expiratory volume in one second (FEV₁) and the forced vital capacity (FVC) are the key values measured. The postbronchodilator ratio of FEV₁ to FVC is crucial in determining the presence of nonreversible airflow limitation, while the postbronchodilator percent predicted value for FEV₁ helps determine the severity of airflow limitation. It's important to note that the ratio of FEV₁ to FVC is not used to assess the severity of airflow limitation because FVC may decrease with increasing obstruction, often due to air trapping or premature termination of exhalation.

GOLD advises utilizing post-bronchodilator readings to diagnose COPD in compliance with national and international criteria. Historically, these values have been preferred for confirming fixed airflow obstruction as they are considered more reproducible, help distinguish COPD from asthma and identify volume responders whose obstruction becomes evident through a bronchodilator-induced increase in FVC. However, practitioners may be discouraged from utilizing spirometry due to the time-consuming aspect of gathering post-bronchodilator data. According to GOLD, pre-bronchodilator spirometry can be performed as a first test to identify airflow limitation in symptomatic patients.

If pre-bronchodilator spirometry does show obstruction, the diagnosis of COPD should be confirmed with post-bronchodilator measurements. Individuals whose pre-bronchodilator FEV₁/FVC ratio is <0.7 but increases to ≥0.7 post-bronchodilator have been found to be at a higher risk of developing COPD in the future and should be closely monitored. GOLD continues to define airflow obstruction in COPD diagnosis as a post-bronchodilator FEV₁/FVC ratio <0.7.

Chest radiography

The chest radiograph demonstrates features of **pulmonary hyperinflation**, characterized by:

- **lung volumes Increased** with low, flattened diaphragms.
- **retrosternal airspace Increased** on the lateral view.
- **Diffuse pulmonary hyperlucency** with attenuation of vascular markings, suggestive of emphysematous changes.
- **Elongation and narrowing of the cardiac silhouette** due to lung overexpansion.
- **Prominent central pulmonary arteries**, likely due to pulmonary hypertension.

Though chest xrays in early COPD patients can be normal and chest xray remains valuable in ruling out alternative diagnoses and complications.

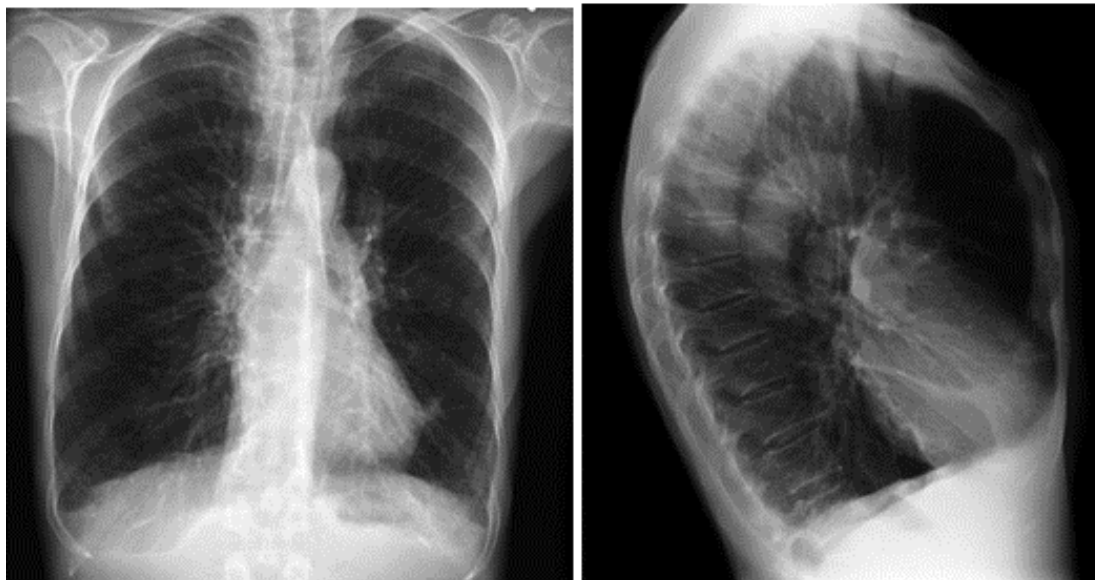


Figure 3: Chest X-ray

Computed tomography

HRCT plays a vital role in the comprehensive evaluation of COPD by providing detailed assessment of parenchymal and airway abnormalities. It helps to visualize and quantify emphysema, air trapping, and airway remodelling, leading to improved phenotyping and management strategies.

Centrilobular Emphysema



Figure 4: Axial HRCT Thorax with centrilobular Emphysema

HRCT thorax axial view lung window showing multiple small low-attenuation areas centered on the respiratory bronchioles with imperceptible walls- centrilobular emphysema with PE may exhibit nonspecific clinical signs of RVD, but several findings can suggest right heart strain.

Paraseptal Emphysema

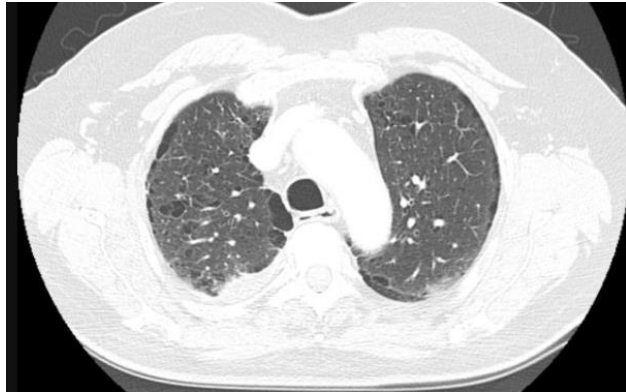


Figure 5: Axial HRCT Thorax with paraseptal Emphysema

HRCT thorax, axial view in lung window showing multiple, predominantly subpleural blebs bilaterally- paraseptal emphysema

Panlobular Emphysema

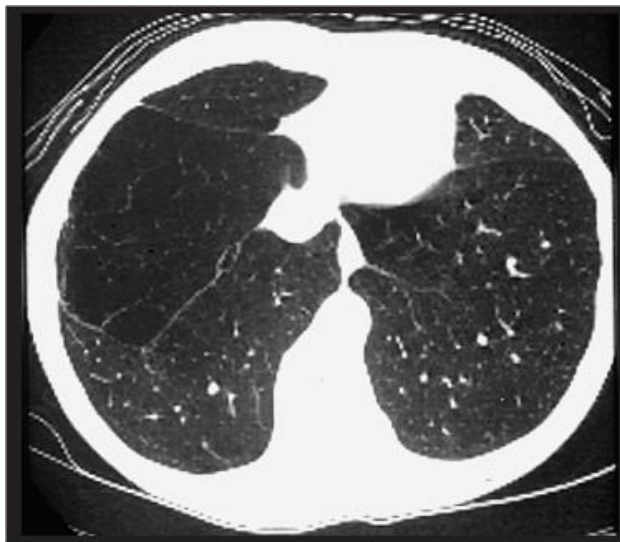


Figure 6: Axial HRCT Thorax with panlobular Emphysema

HRCT thorax axial view, lung window showing diffuse, homogeneous low attenuation with sparse pulmonary vasculature and loss of secondary lobular architecture - Panlobular Emphysema.

Small Airway Disease:

Mosaic attenuation, air trapping on expiratory scans, and centrilobular nodules indicating bronchiolitis.

Chronic Bronchitis:

Airway wall thickening, luminal narrowing, and mucus plugging.

PAST STUDIES

In a study conducted by Nakano Y et al., (2005) to assess the prediction of small airway dimensions using CT. Concluded that CT measurements of airways with a Pi (internal perimeter) of 0.75 cm or more can serve as a reliable method for estimating the dimensions of the small conducting airways, which are the primary sites of airway obstruction in COPD. This suggests that CT imaging could play a crucial role in assessing structural airway changes associated with disease progression and severity in COPD patients.⁴¹

In a cross-sectional study conducted by Gupta PP et al., (2009) to assess high resolution compute tomography features in patients with COPD. Study included total 40 males, showing the tracheal index varied between 0.46 and 0.94, with saber-sheath trachea observed in 14 patients. The mean thoracic cage ratio was 0.69 at the carina level (range 0.61–0.78) and 0.73 at 5 cm below the carina (range 0.62–0.83). The sterno-aortic distance at the carinal level ranged from 1.43 to 4.55 cm, with a mean of 3.00 cm. The most common HRCT finding was directly visible small airways (36 patients), followed by vascular attenuation (25 patients), mosaic attenuation pattern (16 patients), and vascular distortion (8 patients). Among the different subtypes of emphysema, centriacinar emphysema was the most prevalent (16 patients), followed by paraseptal emphysema (13 patients) and panacinar emphysema (11 patients). HRCT provides specific imaging features of emphysema, enabling the identification of subtypes such as centriacinar, panacinar, and paraseptal emphysema. Additionally, hyperinflation-related changes can be effectively identified and quantified using HRCT.⁴²

In a study conducted by Martinez CH et al., (2012) to assess the relationship between quantitative CT metrics and health status and BODE in COPD (n=1200). Both airway disease and emphysema significantly impact clinically relevant outcomes in COPD. Airway measures such as wall thickness (WT), wall area percentage (WA%), and Pi10 were associated with higher SGRQ scores, indicating a stronger influence of airway disease on symptom burden and quality of life. Meanwhile, emphysema had a greater impact on BODE scores, which assess disease severity and prognosis. This suggests that airway disease plays a larger role in patient-reported symptoms, while emphysema more strongly affects overall disease progression and mortality risk.⁴³

Shah A et al., (2014) conducted study to assess the COPD phenotypes according to HRCT scan. Patients with emphysema phenotype on HRCT were more severely affected, with 55% classified as severe COPD according to GOLD guidelines. These individuals demonstrated poor exercise tolerance, with 55% recording a 6MWT distance of less than 250 meters, and 82.5% showed poor bronchodilator reversibility. In contrast, COPD patients with the bronchial wall thickening phenotype also had a high proportion (52%) classified as severe COPD based on GOLD criteria. However, a larger percentage (72.22%) exhibited poor exercise tolerance (6MWT <250m), while 63.88% had poor bronchodilator reversibility. For COPD patients with the bronchiectasis phenotype, the severity was generally moderate (52% as per GOLD guidelines). These patients had better exercise tolerance, with 73.68% achieving a 6MWT distance above 250 meters, and 68.42% displayed good bronchodilator reversibility. However, they experienced a higher frequency of infective exacerbations (52.63%) compared to the other phenotypes. A significant difference was observed when comparing 6MWT among the three phenotypes, with a P-value of 0.016 and an F-value of 4.341. The morphological phenotypes identified through HRCT may aid in predicting COPD severity and determining which patients may benefit from bronchodilator therapy.⁴⁴

Singh A et al., (2016) conducted study to assess correlation between clinical characteristics, spirometric indices and high-resolution CT in COPD. A significant correlation was observed between the smoking index and anteroposterior tracheal diameter ($P = 0.036$). Additionally, the tracheal index decreased with increasing COPD severity, a statistically significant finding ($P = 0.037$). The mean lung density (MLD) values were recorded as -839.27 HU in the upper lobes,

−834.91 HU in the lower lobes, and an overall mean of −837.08 HU, with lower lobe MLD decreasing as disease severity progressed. A mild linear correlation was found between pre-bronchodilator FEV1 and both lower lobe and total average MLD, while post-bronchodilator FEV1 showed correlation with coronal ($P = 0.042$) and sagittal ($P = 0.001$) lower lobe MLD. Furthermore, both pre- ($P = 0.050$) and post- ($P = 0.024$) FEV1/FVC ratios correlated with sagittal lower lobe MLD, suggesting that a predictive model could be developed to quantify obstruction severity (FEV1). HRCT serves as a valuable complementary tool in the comprehensive assessment of COPD, as it correlates well with spirometric and clinical parameters. By measuring MLD, HRCT can indirectly estimate the level of airway obstruction, making it a potentially significant addition to COPD evaluation.⁴⁵

Bhaskar R et al., (2018) conducted study to assess the characteristics of COPD phenotype according to findings on HRCT. A significant correlation was observed between smoking index and anteroposterior tracheal diameter ($P = 0.036$). Additionally, the tracheal index showed a statistically significant decrease with increasing disease severity ($P = 0.037$). A mild linear correlation was noted between pre-FEV1 and both lower lobe and total average MLD, while post-FEV1 exhibited a mild linear correlation with coronal ($P = 0.042$) and sagittal ($P = 0.001$) lower lobe MLD. Furthermore, there was a linear correlation between both pre- ($P = 0.050$) and post- ($P = 0.024$) FEV1/FVC with sagittal lower lobe MLD. These findings highlight the potential role of HRCT as a valuable tool in the comprehensive assessment of COPD, complementing spirometry in evaluating disease severity and structural changes.⁴⁶

Rao P et al., (2018) conducted study to assess HRCT in COPD. Among 50 COPD patients, emphysema predominance was observed in 28 patients (56%), while bronchitis predominance was noted in 19 patients (38%), and 3 patients (6%) exhibited a mixed pattern. Among those with emphysema, the centriacinar pattern was the most common (42.9%), followed by paraseptal (35.71%), bullae (17.8%), and panacinar (3.57%). All patients were chronic smokers with pack years >20, and the entire study group comprised males aged above 45 years. Emphysema was more prevalent in elderly patients over 50 years, whereas chronic bronchitis was primarily seen in those aged 40–50 years. Additionally, 28% of cases had coexisting conditions such as bronchiectasis, lung masses, or interstitial lung disease (ILD). HRCT plays a crucial role in differentiating COPD phenotypes, each of which may require distinct therapeutic approaches.

Furthermore, subtle lung changes that may be missed on chest X-rays can be effectively identified with HRCT, enabling early detection of complications, thereby helping reduce morbidity and mortality.⁴⁷

In a review study conducted by Bodduluri S et al., (2018) to assess the recent advances in CT imaging in COPD. Lung imaging is playing an increasingly important role in the diagnosis, quantification, and phenotyping of COPD. While spirometry remains the gold standard for diagnosing COPD and assessing its severity, CT imaging has gained prominence in both clinical practice and research. COPD is a heterogeneous disease with significant variability in its clinical presentation, radiographic findings, disease progression, and outcomes. Recent studies have highlighted the potential of CT imaging in enhancing diagnostic accuracy, predicting disease progression, refining disease phenotyping, and guiding prognosis. Additionally, CT plays a role in patient selection for targeted interventions and provides valuable insights into the complex pathophysiology of COPD. Several CT-derived metrics have shown promise as imaging biomarkers, offering new opportunities for improved disease assessment and management.⁴⁸

Bhatt SP et al., (2019) conducted study to assess the imaging advances in COPD. Imaging features linked to adverse clinical outcomes in COPD include early interstitial lung abnormalities, emphysema pattern and severity, pulmonary artery-to-aorta diameter ratio, airway wall thickness, and expiratory gas trapping. COPD primarily affects the small conducting airways, and the inclusion of expiratory scans has allowed for a more accurate measurement of small airway disease. Technological advancements in computational imaging have further enabled the indirect assessment of nonemphysematous gas trapping, offering deeper insights into COPD pathogenesis and prognosis, as well as early disease detection. Additionally, several extrapulmonary findings, such as coronary artery calcification, cardiac morphology changes, intrathoracic and extra thoracic fat distribution, and osteoporosis, are now recognized as quantifiable markers of disease burden. Ongoing research is focused on developing novel quantitative imaging biomarkers for emphysema and airway disease, optimizing dose reduction techniques, and leveraging deep learning for advanced COPD phenotyping.⁴⁹

In a study conducted by Vimala LR et al., (2019) to assess the correlation of quantitative and qualitative parameters of HRCT. The presence of inhomogeneous attenuation and the qualitative scoring of emphysema showed the strongest connection with spirometry among the qualitative

measures. The quantitative indicators that shown a substantial connection with spirometry were anterior junction line length, thoracic cage ratio at the aortic arch and inferior pulmonary vein levels, and thoracic cross-sectional area normalized to height at the aortic arch. The tracheal index and anterior junction line length also showed a strong relationship with residual volume/total lung capacity (RV/TLC). The quantitative HRCT and chest X-ray threshold values were found to be lower than those previously reported for the Western population. These results demonstrate how important HRCT is for identifying COPD and estimating the degree of emphysema.⁵⁰

In a review study by Soleeva NB et al., (2022) to assess the CT capabilities in diagnosis of COPD. According to GOLD guidelines, the diagnosis of COPD relies on assessing external respiratory function, with confirmation based on a Tiffno index (FEV1/FVC ratio) below 0.7. However, in the early stages, COPD primarily affects the small bronchi and bronchioles, leading to isolated airway obstruction that may not be detected through spirometry. In such cases, CT serves as the most accurate diagnostic tool, capable of identifying subtle morphological changes associated with early COPD progression.⁵¹

In a study conducted by Zhu D et al., (2022) to assess diagnostic efficacy of visual subtypes and low attenuation area based on HRCT in diagnosis of COPD. As COPD severity worsens, the visual subtypes show a progressive increase ($p < 0.01$). A significant difference in low-attenuation area (LAA) was observed between GOLD stages II–IV and non-COPD individuals ($p < 0.0001$). The diagnostic efficacy of LAA, visual subtypes, and their combination for COPD detection were 0.742, 0.682, and 0.730, respectively. However, when basic patient characteristics were included, the diagnostic efficacy significantly improved to 0.923–0.943 ($p < 0.001$). Based on ROC analysis, an LAA greater than 5.6, worsening of visual subtypes, and positive basic characteristics can help in early identification of potential COPD patients. Given the heterogeneous nature of COPD, a multi-method evaluation approach is essential. The combination of LAA, visual subtypes, and basic characteristics enhances diagnostic accuracy, aligning well with current COPD diagnostic criteria.⁵²

Park J et al., conducted study (2022) to explore the differences in clinical manifestations of COPD patients regarding emphysema distribution along with evidence of airway involvement in chest CT scans in 2022 with 425 individuals which concluded that smoking related COPD

patients with lower dominant emphysema determined by quantitative CT scans had more frequent small and large airway abnormalities than those with upper dominant emphysema, which may be related to the increased risk of exacerbation and better treatment response. Phenotyping COPD patients by emphysema distribution using quantitative CT measurement would be a valuable tool in predicting treatment response and future exacerbation, where the difference in airway involvement severity plays a critical role.⁵³

Rodrigues Sousa S et al., (2024) conducted study to assess COPD phenotype by CT. A total of 80 COPD patients (78.8% male, median age 65 ± 11.3 years) were included in the study. Based on CT phenotyping, patients were classified into normal (31.3percent), air-dominant (33.8percent), emphysema-dominant (21.3percent), and mixed-type (13.8%). The emphysema and mixed phenotypes exhibited the highest ventilatory equivalent for carbon dioxide (V_E/V_{CO_2}) and V_E/V_{CO_2} slope ($p < 0.05$). Across all phenotypes, %LAA showed a positive correlation with V_E/V_{CO_2} and V_E/V_{CO_2} slope. Additionally, % WA was also positively correlated with V_E/V_{CO_2} and V_E/V_{CO_2} slope. In multivariate regression analysis, after adjusting for age, BMI, sex, and FEV1, %LAA remained the only independent predictor of V_E/V_{CO_2} and V_E/V_{CO_2} slope. Emphysema and airway metrics demonstrated strong associations with ventilatory response to exercise in mild to moderate COPD. Notably, %LAA emerged as an independent predictor of V_E/V_{CO_2} and V_E/V_{CO_2} slope, suggesting that CT phenotyping may aid in predicting ventilatory response in COPD patients.⁵⁴

CT Parameter	Measurement Method	Findings
Mean Lung Density (MLD)	HRCT-based lung densitometry (-800 to -1024 HU)	Decreased MLD correlates with increased emphysema severity and FEV1 decline.
Vascular Attenuation	Evaluation of pulmonary vessel thinning	Suggests vascular destruction in emphysematous regions.
Emphysema Severity	Percentage of lung voxels \leq -950 HU on inspiratory CT	correlates with reduced lung function.
Parametric Response Mapping (PRM)	Voxel-wise comparison of inspiratory & expiratory CT scans	Identifies emphysematous vs. small airway disease regions.
Lung Density-Based Disease Progression	Longitudinal HRCT with image registration	Predicts emphysema progression and COPD-related mortality.
Expiratory Gas Trapping (LAA-856exp)	Percentage of lung voxels \leq -856 HU on expiratory CT	More severe air trapping in lower dominant (LD) emphysema patients.

Table 2: Emphysema-Related (quantitative and qualitative) CT Parameters used in various studies

CT Parameter	Measurement Method	Findings
Thoracic Cage Ratio (TCR)	Ratio of AP diameter to transverse diameter	Increased TCR - barrel chest (TCR >0.9)
Sterno-Aortic Distance (SAD)	Distance from posterior sternum to anterior aorta at carina	SAD >4 cm associated with hyperinflation.
Mosaic Attenuation	Alternating high/low attenuation regions on HRCT	Indicates air trapping and small airway dysfunction.
Expiratory-to-Inspiratory Ratio (E/I Ratio)	Mean lung density measured in expiration and inspiration	Higher E/I ratio indicates severe gas trapping and airflow limitation.
Pi10 (Airway Wall Thickness Standardized for Airway Size)	Regression analysis of airway wall thickness	Increased in LD patients, suggesting greater small airway disease.
Airway Wall Thickness (WA%)	Total airway wall area divided by total airway area on HRCT	Higher WA% correlates with COPD severity and frequent exacerbations.
Excessive Central Airway Collapse (ECAC)	% reduction in tracheal area between inspiration & expiration (>50% collapse = ECAC)	Associated with increased dyspnea and poor respiratory quality of life.
Lung Biomechanical Metrics (Jacobian Determinant)	Voxel-based deformation mapping	Lower Jacobian values predict worse airflow limitation and exercise impairment.

Table 3: Hyperinflation (quantitative), small and large airway disease-Related CT Parameters used in various studies

MATERIALS AND METHODS

1. Source of Data:

Patients who are confirmed cases of COPD and patients with clinical suspicion of COPD will be referred from Respiratory medicine and general medicine clinic to department of Radio Diagnosis for HRCT Thorax scan.

2. Study Design

A one-year hospital-based cross-sectional study was conducted.

3. Study Duration

The study was conducted over a one-year period from May 2023 to April 2024.

4. Participants – Inclusion and Exclusion Criteria

Inclusion Criteria

Patients were included in the study based on the following criteria:

1. Age \geq 18 years and $<$ 80 years.
2. Patients with confirmed cases of COPD and patients with clinical suspicion of COPD referred from Respiratory medicine and General medicine clinic to department of Radio Diagnosis.

Exclusion Criteria

Patients were excluded from the study under the following conditions:

1. History of other respiratory illness, including pneumothorax, lung cancer, hydrothorax, destroyed lung, thorax malformation, tuberculosis.

5. Study Sampling

Systemic sampling technique was employed.

6. Sample Size

The sample size was determined based on the following formula:

$$n = \frac{N \times Z_{1-\alpha} \times p \times (100-p)}{d^2 \times (N-1) + Z_{1-\alpha}^2 \times p(100-p)}$$

where N is the estimated COPD HRCT Thorax scans in year= 150

p is prevalence

d estimated error

$Z_{1-\alpha}$ is critical value

$$p = 50\%$$

taking α as 10% $Z_{1-\alpha}$ 1.645

$$d=15\% \text{ of } p= 0.15 \times 50 = 7.5$$

$$n = \frac{150 \times (1.645)^2 \times 50(100-50)}{(7.5)^2 \times (150-1) + (1.645)^2 \times 50(100-50)}$$

$$n = \frac{1014759.37}{8381.25+6765.06}$$

$$8381.25+6765.06$$

$$n=66.9= 67$$

Therefore, the calculated sample size was 67

7. Study Data Collection Procedure

HRCT was performed using a 128-slice CT scanner (General Electronics (GE) Revolution, single-tube machine).

- Scanning was conducted with a field of view large enough to encompass the patient. Images were acquired at full inspiration using 1-mm collimation at 100–120 kV (p) and 90–120 mAs, with a 0.75-second acquisition time.
- Scans were taken at 10-mm intervals with the patient in the supine position, and a slice thickness of 0.6 mm.
- Images were reconstructed using a high spatial frequency algorithm with a 512×512 matrix.
- No contrast was administered.

The following study parameters were evaluated using HRCT:

Tracheal Index: The ratio of the transverse to anteroposterior diameter of the trachea was assessed at a plane 1 cm above the aortic arch in the axial view.

Thoracic Cage Ratio:

Anteroposterior Diameter: The distance from the posterior surface of the sternum to the anterior border of the vertebral body was measured.

Transverse Diameter: The widest horizontal distance between the inner margins of the ribcage at the same axial level was measured.

The ratio of anteroposterior to transverse diameter was evaluated at two anatomical planes:

- At the level of the **tracheal carina**.
- **5 cm below the carina**.

Sterno-Aortic Distance: The distance from the posterior surface of the sternum to the anterior margin of the aorta was measured at the carinal level in the axial images.

Vascular Attenuation: Pulmonary vessel attenuation was noted when there was a reduction in vessel caliber and a decrease in their overall number.

Vascular Distortion: Was noted when an increased branching angle and/or excessive straightening of pulmonary vessels was observed.

Mosaic Attenuation Pattern: Mosaic attenuation was noted when a heterogeneous lung density pattern, with regions of relative lucency interspersed among areas of normal or increased attenuation, was observed.

Directly Visible Small Airways: Airways with an internal diameter of less than 2 mm were noted.

Thoracic Cross-Sectional Area (TCSA): The thoracic cross-sectional area was quantified on HRCT images acquired **1 cm below the top of the aortic arch**. The **TCSA-to-height² ratio (TCSAcm²/height² in metre)** was subsequently calculated for each patient.

Low attenuation areas of emphysema were assessed on HRCT and were classified into **centrilobular emphysema**, (when focal areas of decreased attenuation with no discernable wall are found in association with respiratory bronchioles are present) **panlobular emphysema** (when large areas of decreased lung density with poorly - defined margins and enlarged air spaces are evenly distributed within and across acinar units) and **paraseptal emphysema** (when the enlarged air spaces were seen along the edge of the acinar unit abutting pleura or a vessel).

12. Ethical Considerations

Institutional Ethical Clearance was obtained from the Institutional Ethics Committee for Human Subjects Research of Jawaharlal Nehru Medical College, Belagavi, Karnataka.

Institutional Ethical Clearance Ref No. MDC/JNMCIEC/201

Participants were provided informed written consent, and only those willing to sign the consent form were included in the study. Before obtaining consent, participants were informed about the risks and benefits associated with the research, as well as the voluntary nature of their participation. The confidentiality of all participants was strictly maintained throughout the study. The patient's data were collected in pre-designed, pre-tested questionnaire to collect the demographic details and medical history.

ANALYSIS AND RESULTS

Analysis

All the data were entered in excel sheet and analysed using SPSS v26.0 operating on windows 10. The data were summarised as mean, standard deviation, frequency and percentage. The summarised data were represented with tables, figures, bar diagram, and pie chart. The categorical data were compared using chi-square test. A p-value of <0.05 was considered statistically significant.

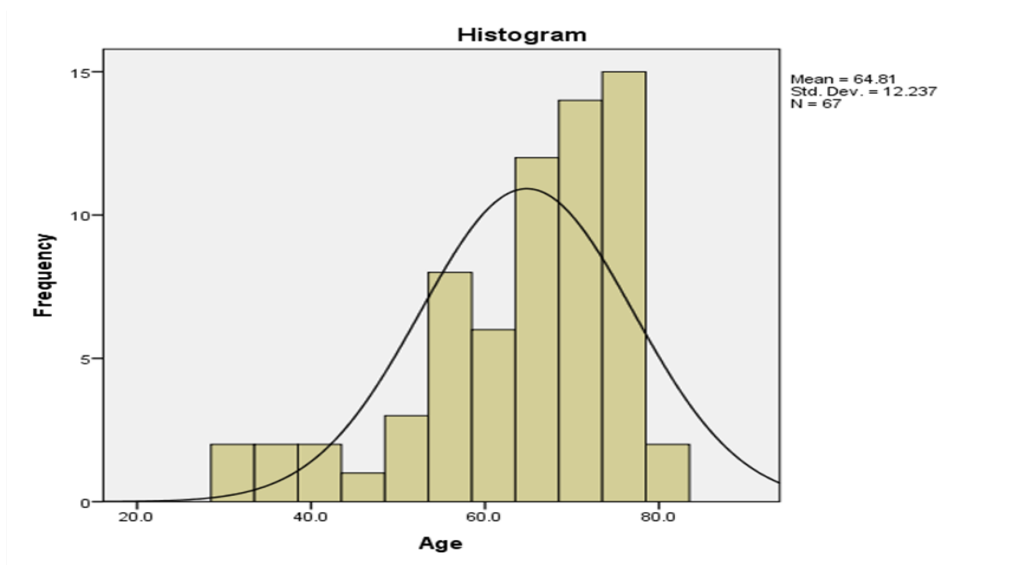
Results

The table showing **age distribution** of the study population. The sample includes **67 participants**, with ages ranging from **31 to 79 years**. The **mean age** of participants is **64.65 years**, with a **standard deviation (SD) of 12.66**, indicating a moderate spread of ages around the mean.

Table 2: Gender Distribution of the Study Population

	N	Minimum	Maximum	Mean	SD
Age in years	67	31.0	79.0	64.65	12.66

Table 4: Demographic characteristics of study population



Graph 1 : Demographic characteristics of study population

Analysis and Results

		Count	N %
Gender	Female	14	20.9%
	Male	53	79.1%

Table 5: Gender distribution of study population

The table presents the **gender distribution** of the study population. **Males** constituted the majority, accounting for **79.1%** of the cases, while **females** comprised **20.9%**. This indicates a higher prevalence of COPD among males, which may be attributed to factors such as **higher smoking rates and occupational exposure to pollutants**. However, the presence of COPD in females suggests that other risk factors, including **biomass fuel exposure and genetic predisposition**, may also play a role.

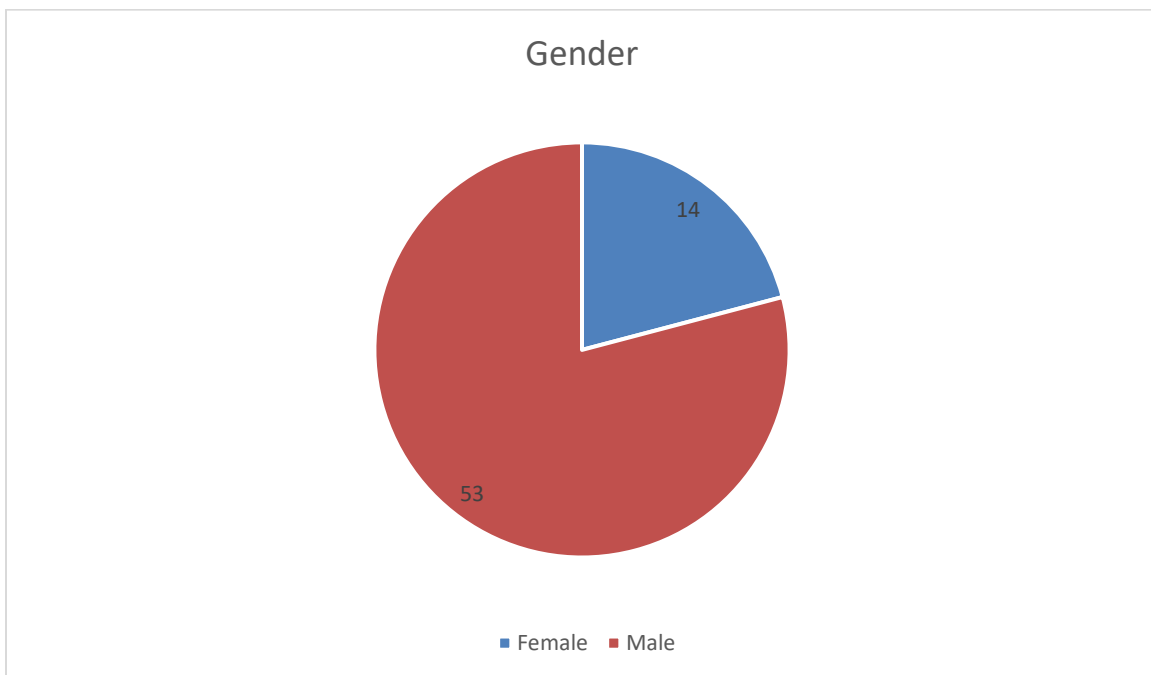


Figure 7: Gender distribution among study population

Analysis and Results

		Count	N %
Family history	Asthma	1	1.5%
	COPD	2	3.0%
	NAD	64	95.5%
Smoking history	Absent	17	25.4%
	Present	50	74.6%
Physical examination	Barrel chest	3	4.5%
	Wheeze	1	1.5%
	No Wheeze / Barrel chest	63	94.0%
Respiratory system	Crepts	4	6.0%
	NVBS	60	89.6%
	NVBS with scattered crepts	1	1.5%
	Rhonchi	1	1.5%
	VBS	1	1.5%

Table 6: Demonstrating family history, smoking history and physical examination

The table presents data on **family history, smoking history, and physical examination findings** in COPD patients. A **family history of COPD** was reported in **3.0%** of cases, while **1.5%** had a family history of asthma. However, the majority (**95.5%**) had **no abnormal findings (NAD)** related to family history.

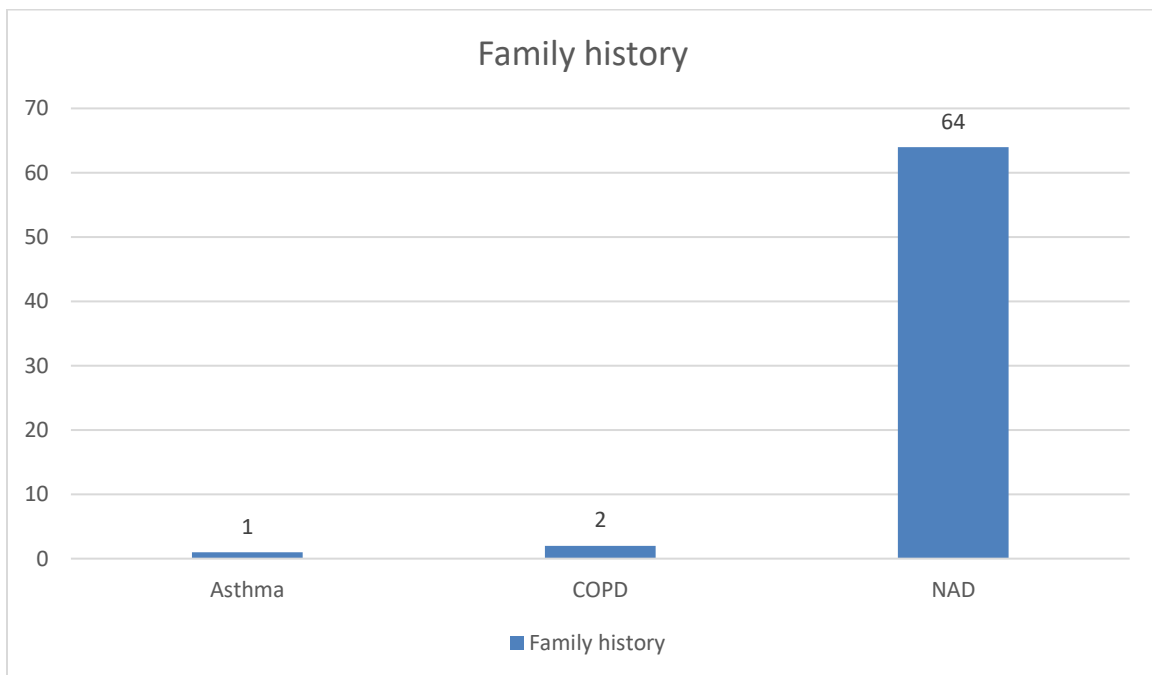
Regarding **smoking history**, **74.6%** of patients had a **history of smoking**, while **23.9%** had never smoked. Only **1.5%** had missing smoking data.

On **physical examination**, **94.0%** of patients had findings within normal limits (WNL). However, **barrel chest** was observed in **4.5%** and **wheezing** in **1.5%** of cases. These findings

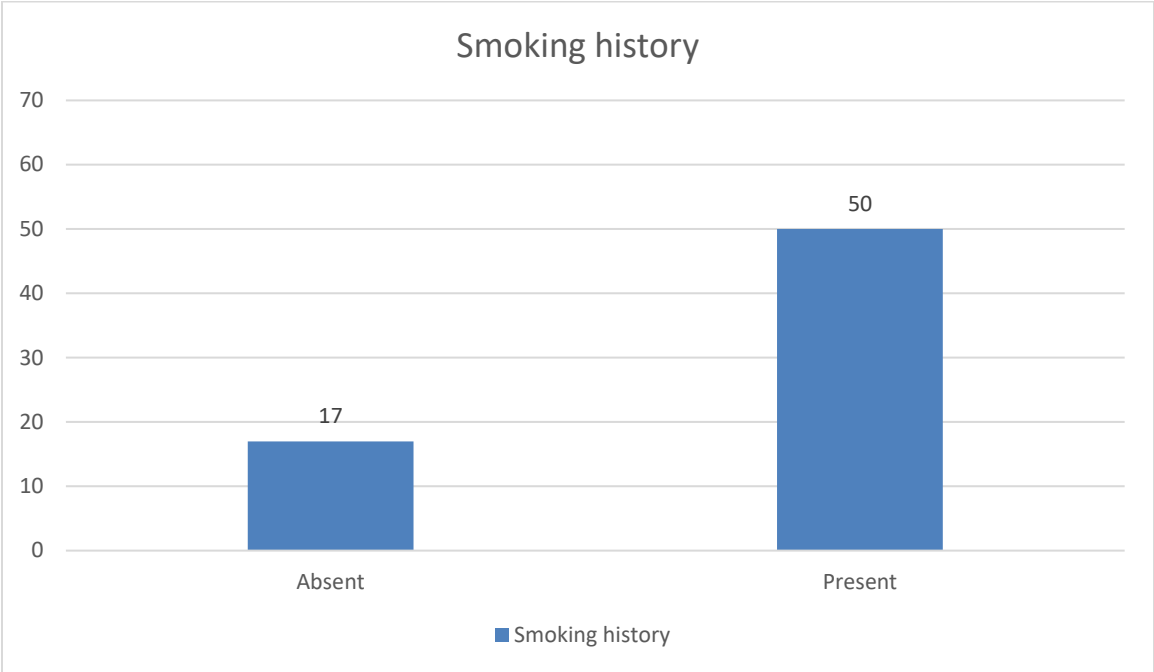
Analysis and Results

suggest that while physical examination may be normal in most COPD cases, some patients exhibit signs of **chronic airflow limitation and hyperinflation**.

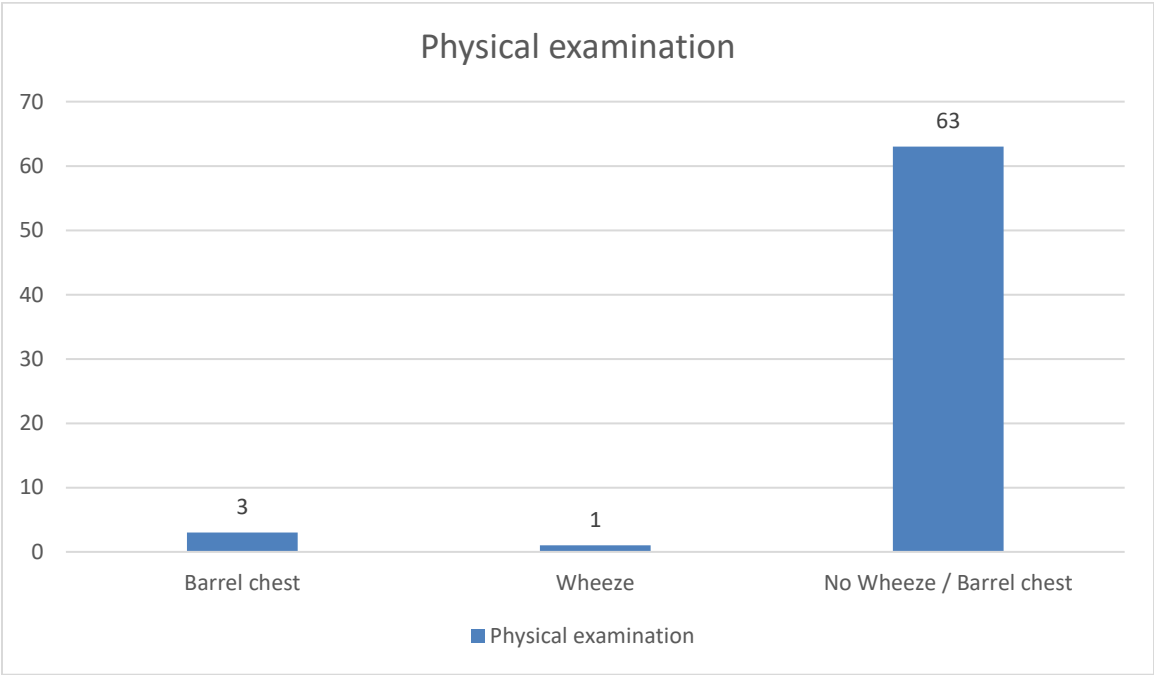
The table also presents findings related to **respiratory system (RS) auscultation** in COPD patients. The majority of patients (**89.6%**) had **normal vesicular breath sounds (NVBS)**, while various types of **crepitations (crackles)** were observed in a small percentage of cases, including **bilateral basal crepts, bilateral crepts, scattered crepts, and general crepts** (each **1.5%**). **Rhonchi** and **vesicular breath sounds (VBS)** were also noted in **1.5%** of cases each.



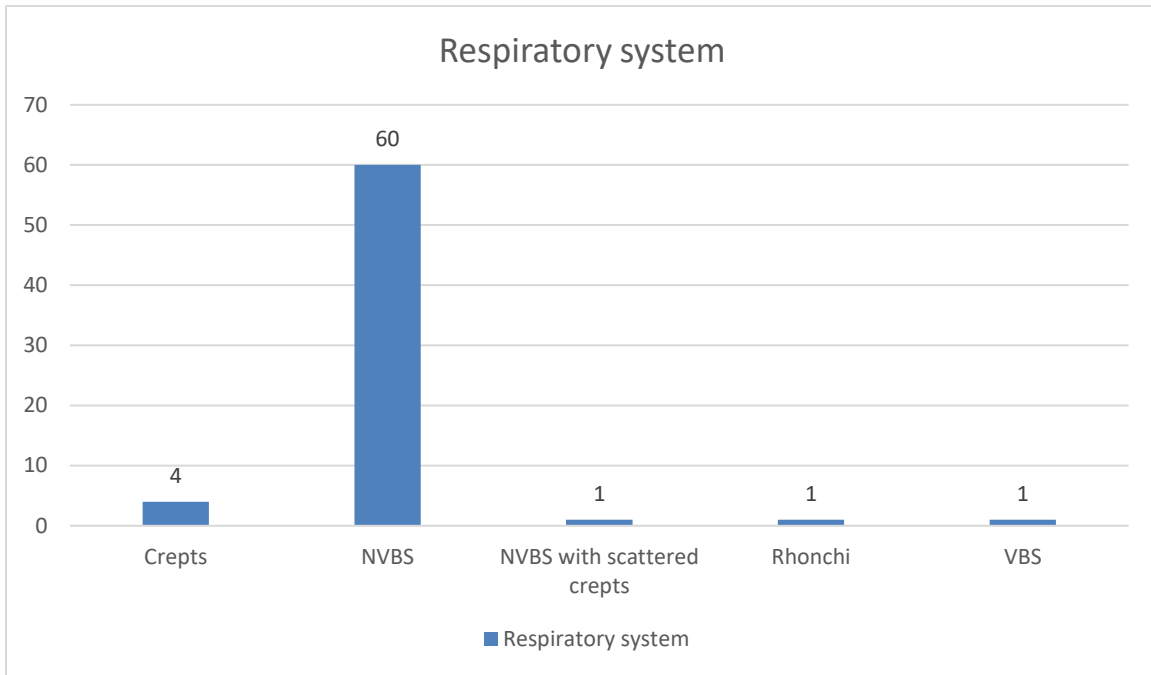
Graph 2: Bar graph representing family history



Graph 3 : bar graph representing presence of smoking history



Graph 4 : Bar graph representing findings of physical examination



Graph 5: Bar chart demonstrating the findings of respiratory system examination

	Mean	SD
FEV ₁	58.71	10.71
FVC	84.19	16.76
FEV ₁ /FVC	.68	.06
FEF _{25-75%}	45.3	13.7
PEFR	49.5	16.8

Table 1: Spirometry measurements of the study population

The table presents spirometry measurements, providing an overview of pulmonary function among the study population. The mean Forced Expiratory Volume in 1 second (FEV₁) was 58.71 ± 10.71, indicating a moderate reduction in expiratory airflow. The Forced Vital Capacity (FVC) had a mean of 84.19 ± 16.76, suggesting relatively preserved lung capacity. The FEV₁/FVC ratio

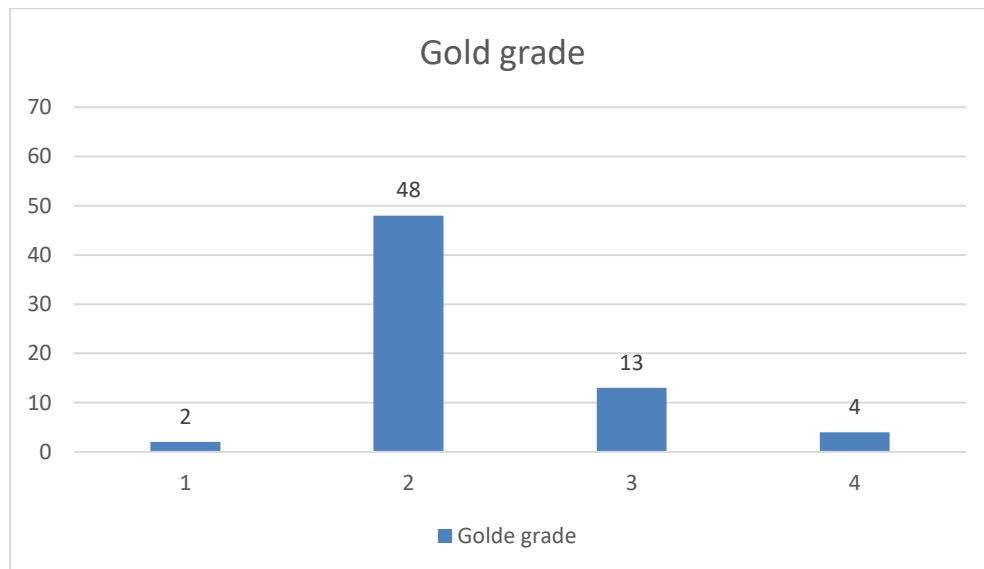
Analysis and Results

averaged 0.68 ± 0.06 , which is lower than the normal threshold, indicative of obstructive airway disease. The Forced Expiratory Flow at 25–75% (FEF_{25–75%}) was 45.3 ± 13.7 , reflecting small airway dysfunction. Additionally, the Peak Expiratory Flow Rate (PEFR) was 49.5 ± 16.8 , further supporting airflow limitation.

		Count	N %
Gold Grade	1.0	2	3.0%
	2.0	48	71.6%
	3.0	13	19.4%
	4.0	4	6.0%

Table 8: Gold grade of study population

Tables showing the **GOLD grades**, most patients were classified as **GOLD 2 (71.6%)**, followed by **GOLD 3 (19.4%)**, and a small proportion in **GOLD 4 (6.0%)**. Only **3.0%** of patients were in **GOLD 1**, indicating that moderate COPD (GOLD 2) was the most prevalent severity level.



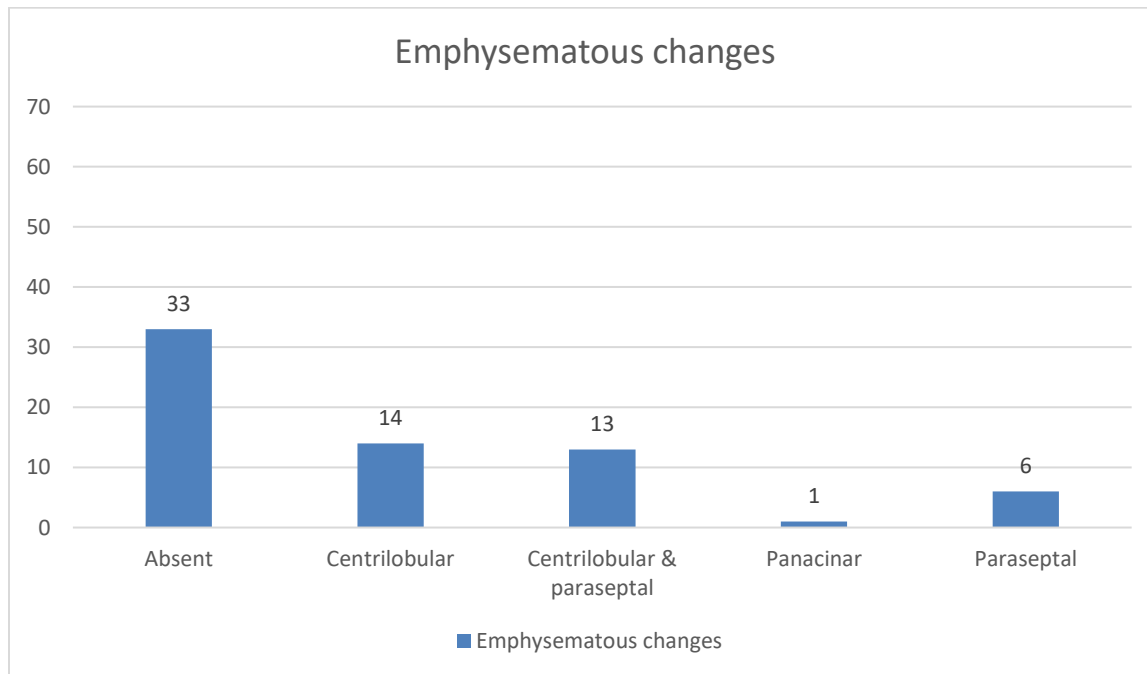
Graph 6: Bar chart demonstrating the distribution according to Gold grade

Analysis and Results

		Count	N %
Emphysematous changes	Absent	33	49.3%
	Centrilobular	14	20.9%
	Centrilobular & paraseptal	13	19.4%
	Panacinar	1	1.5%
	Paraseptal	6	9.0%

Table 2: Distribution of emphysematous changes

In present study **emphysematous changes**, nearly half of the patients (**49.3%**) had no emphysema. Among those with emphysema, **centrilobular emphysema** was the most common type (**20.9%**), followed by **centrilobular & paraseptal emphysema** (**19.4%**). **Paraseptal emphysema** was seen in **9.0%**, while **panacinar emphysema** was the least frequent, affecting only **1.5%** of patients.



Graph 7: bar graph demonstrating the distribution of Emphysematous changes

	Mean	SD
Thoracic index	0.98	0.21
Thoracic cage ratio at carina	0.51	0.31
Thoracic cage ratio 5cm below carina	0.55	0.28
Sterno aortic distance in cm	2.26	1.03
Thoracic cross-sectional area /height sq (cm/msq)	81.0	37.8

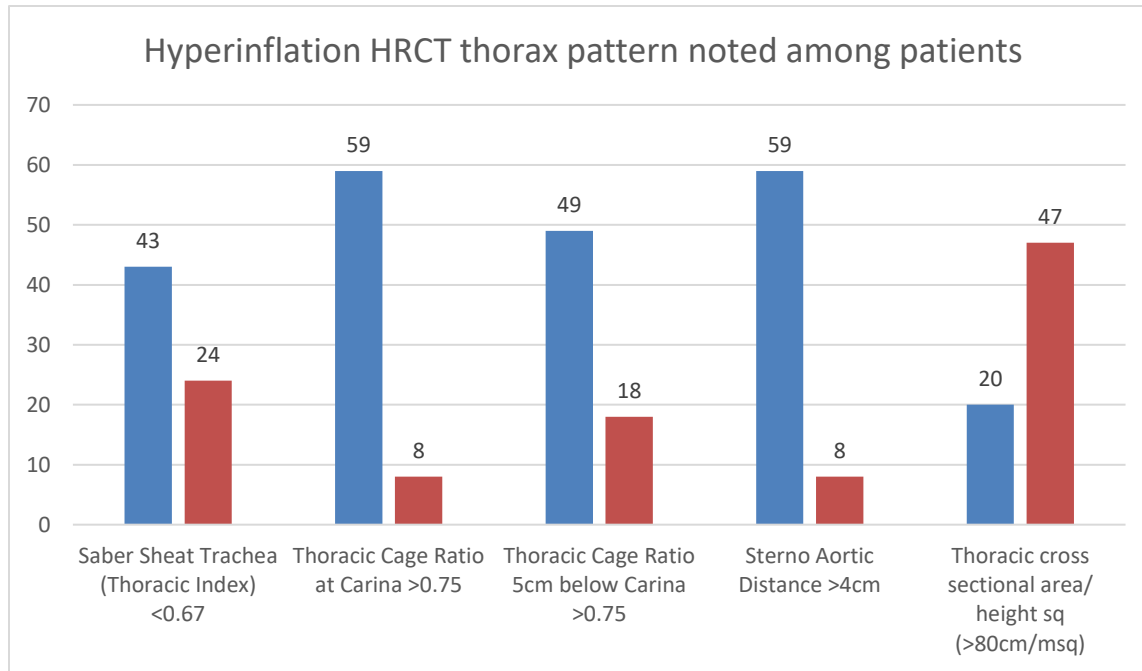
Table 3: Quantitative HRCT measurement for hyperinflation

The table presents HRCT measurements related to thoracic morphology. The mean thoracic index was 0.98 ± 0.21 , reflecting the shape and dimensions of the trachea. The thoracic cage ratio at the level of the carina had a mean of 0.51 ± 0.31 , while 5 cm below the carina, it was slightly higher at 0.55 ± 0.28 , indicating variations in thoracic cage dimensions at different levels. The sterno-aortic distance averaged 2.26 ± 1.03 cm, which provides insight into the retrosternal space. Lastly, the thoracic cross-sectional area normalized to height had a mean value of 81.0 ± 37.8 cm/m², reflecting differences in overall thoracic dimensions among patients. These measurements help in assessing thoracic structural variations and their potential clinical significance.

		Count	N %
Saber Sheat Trachea (Thoracic Index) <0.6	No	43	64.2%
	Yes	24	35.8%
Thoracic Cage Ratio at Carina >0.75	No	59	88.1%
	Yes	8	11.9%
Thoracic Cage Ratio 5cm below Carina >0.75	No	49	73.9%
	Yes	18	26.1%
Sterno Aortic Distance >4cm	No	59	88.1%
	Yes	8	11.9%
Thoracic cross sectional area/ height sq (>80cm/msq)	No	20	29.8%
	Yes	47	70.2%

Table 4: Hyperinflation pattern of HRCT thorax.

Saber Sheath Trachea (Thoracic Index <0.67) was observed in 35.8% of cases. Thoracic Cage Ratio at Carina >0.75 was noted in 11.9% of patients, while the same ratio 5 cm below the carina was slightly higher at 26.1%. Sterno-Aortic Distance >4 cm was found in 11.9% of cases. Lastly, an increased Thoracic Cross-Sectional Area/Height² (>80 cm/m²) was seen in 70.2% of patients. These findings highlight variations in thoracic morphology among the study population.

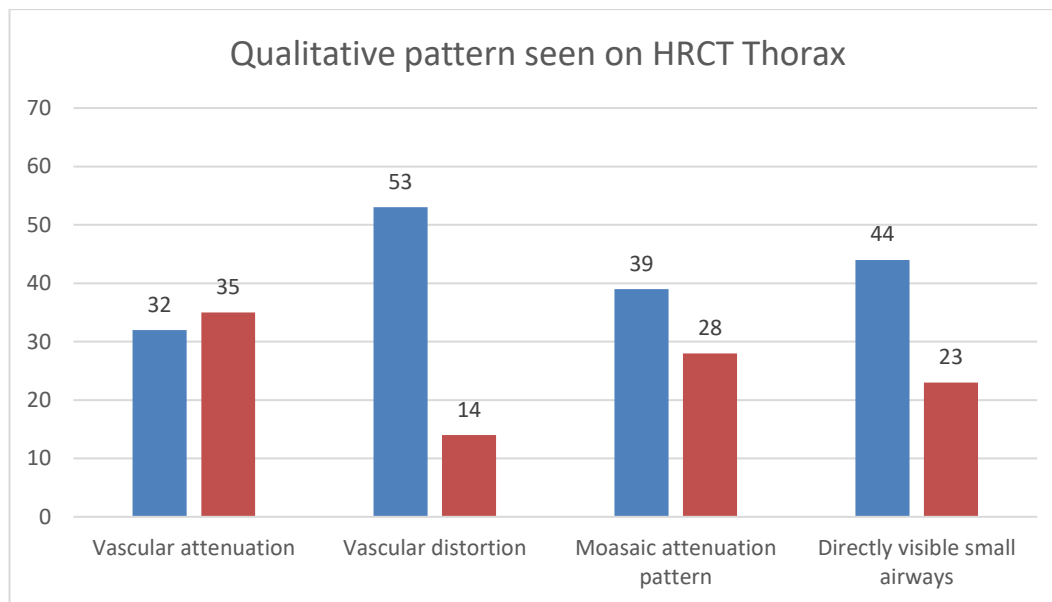


Graph 8 : Bar chart demonstrating quantitative HRCT thorax pattern for hyperinflation noted among patients

		Count	N %
Vascular attenuation	Absent	32	47.8%
	Present	35	52.2%
Vascular distortion	Absent	53	79.1%
	Present	14	20.9%
Moasaic attenuation pattern	Absent	39	58.2%
	Present	28	41.8%
Directly visible small airways	Absent	44	65.7%
	Present	23	34.3%

Table 5: Qualitative pattern emphysema and hyperinflation seen on HRCT Thorax

The table presents the **prevalence of vascular and airway abnormalities in COPD patients**. **Vascular attenuation** was observed in **52.2%** of cases, while **47.8%** showed no attenuation, indicating a nearly equal distribution. **Vascular distortion** was less common, with **20.9%** of patients exhibiting this feature, while **79.1%** had no distortion. The **mosaic attenuation pattern** was present in **41.8%** of patients, suggesting a significant proportion with heterogeneous lung perfusion, whereas **58.2%** did not show this feature. **Directly visible small airways** were noted in **34.3%** of cases, while **65.7%** showed no such findings.



Graph 9 : Bar graph demonstrating qualitative pattern for emphysema and hyperinflation seen on HRCT Thorax

	Gold Grade								p-value
	1.0		2.0		3.0		4.0		
	Mean	SD	Mean	SD	Mean	SD	Mean	SD	
Thoracic index	0.98	0.11	0.85	0.22	0.75	0.15	0.6	0.07	0.05*
Thoracic cage ratio at carina >0.75	0.45	0.08	0.46	0.36	0.5	0.07	0.54	0.09.	0.26
Thoracic cage ratio 5cm below carina >0.75	0.51	0.03	0.54	0.32	0.56	0.11	0.62	0.1	0.05*
Sterno aortic distance in cm	2.16	0.35	2.22	0.99	3.15	1.20	3.50	1.32.	0.05*
Thoracic cross sectional area /height sq (cm/msq)	71.5	20.5	73.9	29.3	82.5	62.3	120.3	22.3.	0.05*

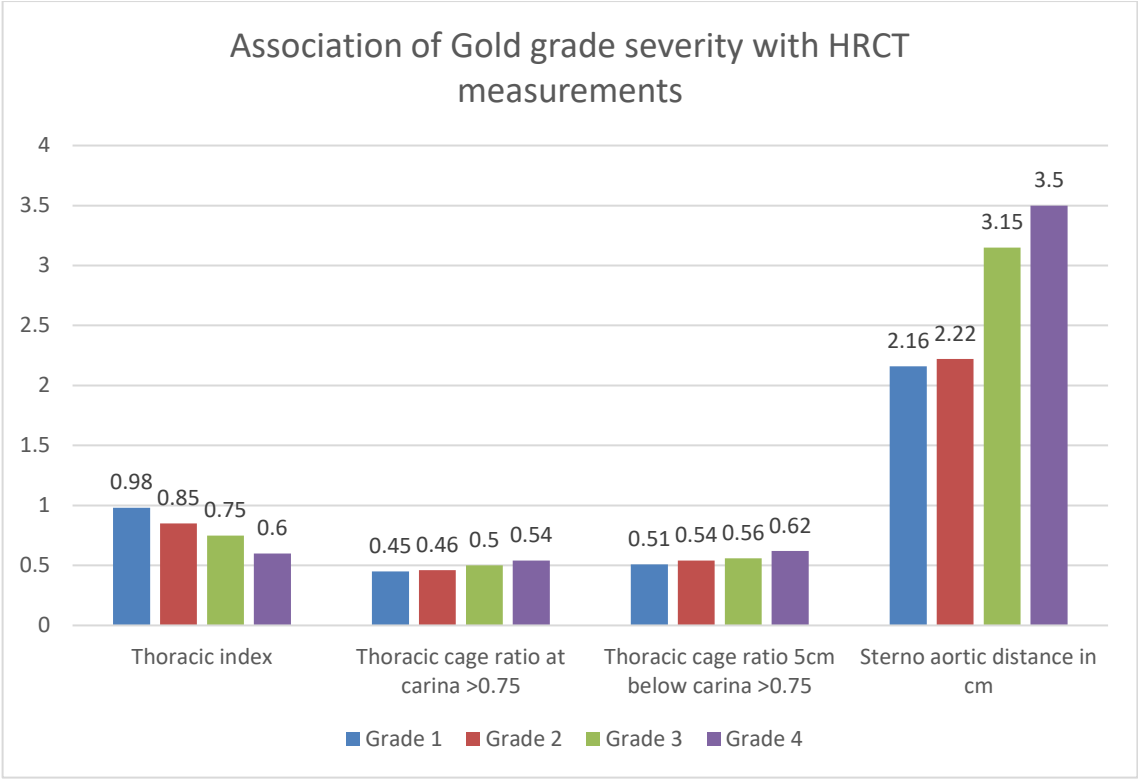
Table 6: Association of Gold grade severity with quantitative HRCT hyperinflation patterns

The analysis of the association between GOLD grade severity and HRCT measurements reveals significant trends across various thoracic parameters.

The thoracic index demonstrated a statistically significant decrease with GOLD grade severity, showing a mean value of 0.6 (SD = 0.07) in GOLD 1, progressively rising to 0.98 (SD = 0.11) in GOLD 4 ($p = 0.05$). This suggests that worsening airflow limitation is associated with an increase in thoracic index, potentially reflecting structural changes in the thorax due to disease progression. Similarly, the thoracic cage ratio measured 5 cm below the carina exhibited a gradual increase from 0.51 (SD = 0.03) in GOLD 1 to 0.62 (SD = 0.1) in GOLD 4, with a significant association ($p = 0.05$). This finding indicates progressive thoracic cage expansion in response to increasing disease severity. However, the thoracic cage ratio at the level of the carina did not show a statistically significant correlation with GOLD grade severity ($p = 0.26$), suggesting that changes in this parameter may not be as strongly linked to disease progression.

The sterno-aortic distance significantly increased with GOLD severity, ranging from 2.16 cm (SD = 0.35) in GOLD 1 to 3.50 cm (SD = 1.32) in GOLD 4 ($p = 0.05$). This increase likely reflects hyperinflation and anterior displacement of the sternum, commonly observed in advanced chronic obstructive pulmonary disease (COPD). Lastly, the thoracic cross-sectional area adjusted for height exhibited a marked increase with GOLD severity, from a mean of 71.5 cm²/msq (SD = 20.5) in GOLD 1 to 120.3 cm²/msq (SD = 22.3) in GOLD 4, with a statistically significant association ($p = 0.05$). This suggests that increased thoracic expansion is a characteristic feature of more severe COPD cases.

Overall, these findings indicate that HRCT-based thoracic measurements, particularly the thoracic index, thoracic cage ratio (5 cm below carina), sterno-aortic distance, and thoracic cross-sectional area, are significantly associated with GOLD grade severity and could serve as valuable imaging markers in COPD assessment.



Graph 10 : Bar graph demonstrating association of Gold grade severity with quantitative HRCT thorax measurements

DISCUSSION

COPD is a progressive and debilitating respiratory disorder characterized by airflow limitation and persistent respiratory symptoms. It encompasses conditions such as chronic bronchitis and emphysema, which significantly impact lung function and quality of life. Accurate assessment and early detection of structural lung changes are crucial for effective management, and imaging plays a vital role in this process.¹ HRCT of the thorax has emerged as an essential tool in evaluating COPD, providing detailed visualization of pulmonary abnormalities that are not always apparent on conventional radiography or pulmonary function tests.^{43,47,54}

HRCT enables precise characterization of various imaging patterns associated with COPD, including emphysematous changes, bronchial wall thickening, air trapping, and small airway disease. It helps differentiate between different phenotypes of COPD, which can influence treatment decisions and prognostic outcomes.⁵² The ability of HRCT to detect early structural alterations in the lungs also aids in assessing disease severity and progression, offering valuable insights beyond spirometric evaluation.

Furthermore, HRCT plays a significant role in identifying complications and coexisting conditions, such as bronchiectasis, interstitial lung abnormalities, and pulmonary hypertension, which can impact clinical management. Quantitative analysis of lung density and texture using HRCT allows for objective assessment of emphysema extent, aiding in risk stratification and therapeutic planning.^{8,10} The evolving role of artificial intelligence and machine learning in HRCT interpretation has further enhanced diagnostic accuracy and efficiency.⁵

The sample includes 67 participants, with mean age is 64.65 ± 12.66 years, with 20.9% were female and 79.1% were male, showing the male preponderance. Family history of COPD was present in 3%, smoking present in 74.6% and on physical examination showing barrel chest in 4.5%.

In similar study by Rao P et al. (2018) reported that all their study participants were chronic smokers with more than 20 pack-years of exposure, and their cohort consisted entirely of males above 45 years. This aligns with the male preponderance and high smoking prevalence in the

current study.⁴⁷ In study by Singh A et al., the mean age of patients was 58.43±9.72yrs with male preponderance. Among them 88.57% were smokers with mean pack years was 22.76.⁴⁵

In present study, the spirometry measurements showing the mean Forced Expiratory Volume in 1 second (FEV₁) was 58.71 ± 10.71, indicating a moderate reduction in expiratory airflow. The Forced Vital Capacity (FVC) had a mean of 84.19 ± 16.76, suggesting relatively preserved lung capacity. The FEV₁/FVC ratio averaged 0.68 ± 0.06, which is lower than the normal threshold, indicative of obstructive airway disease. The Forced Expiratory Flow at 25–75% (FEF_{25–75%}) was 45.3 ± 13.7, reflecting small airway dysfunction. Additionally, the Peak Expiratory Flow Rate (PEFR) was 49.5 ± 16.8, further supporting airflow limitation.

	Vimala LR et al., ⁵⁰	Present study
FVC	77.68	84.19
FEV1%	54.33	58.71
FEV1/FVC	54.96	68.65
PEFR	64.47	49.5

Table 7: Comparison of spirometry values with previous studies

In a similar to present study by Vimala LR et al. presents pulmonary function test (PFT) values indicative of moderate obstructive lung disease. The forced vital capacity (FVC) is reported at 77.68%, suggesting a mild reduction in lung volume, which could be associated with either restrictive or obstructive lung disease. The forced expiratory volume in one second (FEV1%) is 54.33%, indicating a significant decline in expiratory airflow, which is a hallmark of moderate airflow obstruction. Furthermore, the FEV1/FVC ratio is 54.96%, which is well below the normal threshold of 70%, confirming an obstructive ventilatory pattern commonly seen in COPD or asthma. Additionally, the PEFR is 64.47%, reflecting a moderate impairment in the ability to expel air quickly, further supporting the diagnosis of an obstructive lung condition.⁵⁰

COPD Gold grade, showing presence of grade 2 in 76.1%, followed by 19.4% with grade 3, 3% with grade 1 and 1.5% with grade 4 GOLD criteria. Emphysematous changes was present in

50.7% with majority showing the centrilobular changes in 20.9% and 19.4% with centrilobular and paraseptal changes.

	Vimala LR et al., ⁵⁰	Present study
Centrilobular	18%	20.9%
Panacinar	29%	1.5%
Paraseptal	6%	9.0%
Combined Centrilobular & paraseptal	16%	19.4%

Table 8: Comparison of emphysematous changes with previous studies

In similar study by Gupta PP et al. (2009) observed centriacinar emphysema as the most common type (16 patients), followed by paraseptal and panacinar emphysema. The prevalence rates in their study align with the present findings.⁴² Rao P et al. (2018) reported a predominance of centriacinar emphysema and bronchitis phenotypes, paralleling the emphysema and bronchiectasis prevalence in the current study. Among those with emphysema, the centriacinar pattern was the most common (42.9%), followed by paraseptal (35.71%), bullae (17.8%), and panacinar (3.57%).⁴⁷

	Gupta PP et al. ⁴²	Present study
Saber Sheat Trachea (Thoracic Index)	35%	35.8%
Thoracic Cage Ratio at Carina >0.75	12.5%	11.9%
Thoracic Cage Ratio 5cm below Carina >0.75	27.5%	26.1%
Sterno Aortic Distance >4cm	12.5%	11.9%
Thoracic cross- sectional area/ height sq (>80cm/msq)	70%	70.2%

Table 9: Comparison of quantitative measurement with previous studies

The study by Gupta PP et al. reported various thoracic structural changes associated with emphysema. The most common finding was an increased thoracic cross-sectional area-to-height

ratio (>80 cm/m²) in 70% of cases, followed by Saber Sheath Trachea (thoracic index) in 35%. A thoracic cage ratio greater than 0.75 was observed in 27.5% of cases at 5 cm below the carina and in 12.5% at the carina level. Additionally, an increased sterno-aortic distance (>4 cm) was noted in 12.5% of cases. These findings highlight significant thoracic remodeling in emphysematous patients, which may have clinical implications for disease severity and management.⁴²

	Gupta PP et al. ⁴²	Singh A et al. ⁴⁵	Present study
Vascular Attenuation	62.5%	88.5%	52.2%
Vascular Distortion	20%	6.5%	20.9%
Mosaic Attenuation Pattern	40%	22.85%	41.8%
Directly Visible Small Airways	90%	45.3%	34.3%

Table 10: Comparison of qualitative patterns with previous studies

Gupta PP et al. (2009) found vascular attenuation in 25 patients and mosaic attenuation in 16 patients, which supports the presence of these findings in COPD patients. In the present study vascular attenuation was seen in 52.2%, vascular distortion in 20.9%, mosaic attenuation pattern in 41.8% and directly visible small airways in 34.3% of the cases

HRCT provides specific imaging features of emphysema, enabling the identification of subtypes such as centriacinar, panacinar, and paraseptal emphysema. Additionally, hyperinflation-related changes can be effectively identified and quantified using HRCT.⁴² Singh A et al. (2016) and Bhaskar R et al. (2018) found a significant correlation between HRCT-derived mean lung density (MLD) and COPD severity.⁴⁵

Soleeva NB et al. (2022) emphasized the importance of CT in diagnosing early-stage COPD, where spirometry might not detect small airway obstruction. This supports the finding that directly visible small airways were observed in 34.3% of cases in the current study.⁵¹

Rodrigues Sousa S et al. (2024) found emphysema-dominant and mixed phenotypes to be associated with a higher ventilatory equivalent for carbon dioxide (VE/VCO₂), linking CT phenotyping with exercise limitations. While the present study did not assess ventilatory responses, the HRCT phenotypic categorization aligns with their finding.⁵⁴

The analysis of the association between GOLD grade severity and HRCT measurements reveals significant trends across various thoracic parameters.

The thoracic index demonstrated a statistically significant decrease with GOLD grade severity, the thoracic cage ratio measured 5 cm below the carina exhibited a gradual increase from 0.51 (SD = 0.03) in GOLD 1 to 0.62 (SD = 0.1) in GOLD 4, with a significant association ($p = 0.05$). This finding indicates progressive thoracic cage expansion in response to increasing disease severity. However, the thoracic cage ratio at the level of the carina did not show a statistically significant correlation with GOLD grade severity.

CONCLUSION

HRCT plays a crucial role in assessing imaging patterns in COPD. This study, conducted on 67 participants with a male predominance (79.1%) and a mean age of 64.65 years, highlights the significance of HRCT in identifying structural abnormalities associated with COPD severity. Emphysematous changes were present in 50.7%, predominantly centrilobular and combined centrilobular-paraseptal types. HRCT findings such as vascular attenuation (52.2%), vascular distortion (20.9%), mosaic attenuation pattern (41.8%), and directly visible small airways (34.3%) were documented. The thoracic measurements showed a statistically significant correlation with disease severity. While HRCT provides valuable insights into structural lung changes in COPD, further research with larger sample sizes is required to establish definitive associations with disease progression.

SUMMARY

- The sample includes 67 participants, with ages ranging from 31 to 79 years. The mean age is 64.65 years, with a standard deviation (SD) of 12.66, indicating a moderate spread of ages around the mean.
- Among them 20.9% were female and 79.1% were male with male preponderance.
- Family history of COPD was present in 3%, smoking present in 74.6% and on physical examination showing barrel chest in 4.5%.
- COPD Gold grade, showing presence of grade 2 in 76.1%, followed by 19.4% with grade 3, 3% with grade 1 and 1.5% with grade 4 GOLD criteria.
- Emphysematous changes was present in 50.7% with majority showing the centrilobular changes in 20.9% and 19.4% with centrilobular and paraseptal changes.
- Saber Sheath Trachea (Thoracic Index <0.67) was observed in 35.8% of cases. Thoracic Cage Ratio at Carina >0.75 was noted in 11.9% of patients, while the same ratio 5 cm below the carina was slightly higher at 26.1%. Sterno-Aortic Distance >4 cm was found in 11.9% of cases. Lastly, an increased Thoracic Cross-Sectional Area/Height² (>80 cm/m²) was seen in 70.2% of patients. These findings highlight variations in thoracic morphology among the study population.
- On HRCT, vascular attenuation was seen in 52.2%, vascular distortion in 20.9%, mosaic attenuation pattern in 41.8% and directly visible small airways in 34.3% of the cases.
- HRCT Thoracic measurements across GOLD grades of COPD severity, showing statistically significant differences. The thoracic cage ratio and sterno-aortic distance showed minimal variation, with p-values indicating significant association with disease severity. Notably, thoracic cross-sectional area/height squared increased in GOLD 4. Overall, trends were observed with thoracic parameters demonstrating a strong association with COPD severity.

STRENGTHS

- This study on the role of high-resolution computed tomography (HRCT) in assessing various imaging patterns in chronic obstructive pulmonary disease (COPD) has several strengths.
- Firstly, HRCT is a highly sensitive imaging modality that provides detailed visualization of lung parenchymal changes, enabling precise classification of emphysema subtypes and small airway involvement.
- The study's structured methodology, including a well-defined inclusion and exclusion criteria, ensures the reliability of findings by focusing specifically on COPD cases and minimizing confounding factors.
- Additionally, the use of standardized parameters such as tracheal index, thoracic cage ratio, sterno-aortic distance and thoracic cross sectional area enhances the objectivity of imaging assessment.
- The ethical considerations, including informed consent and strict confidentiality measures, further add to the study's credibility.

LIMITATIONS

- The study is hospital-based and cross-sectional in design, limiting its generalizability to broader populations.
- The relatively small sample size of 67 patients may not fully represent the diversity of COPD presentations.
- Lastly, potential inter-observer variability in interpreting HRCT findings may influence diagnostic accuracy, despite standardized imaging protocols.

BIBLIOGRAPHY

1. Singh D, Agusti A, Anzueto A, Barnes PJ, Bourbeau J, Celli BR, et al. Global Strategy for the Diagnosis, Management, and Prevention of Chronic Obstructive Lung Disease: the GOLD science committee report 2019. *Eur Respir J*. 2019;53(5):11–22.
2. Parris BA, O’Farrell HE, Fong KM, Yang IA. Chronic obstructive pulmonary disease (COPD) and lung cancer: common pathways for pathogenesis. *J Thorac Dis Vol 11, Suppl 17 (October 31, 2019) J Thorac Dis (Advances Multidiscip Care COPD)*. 2019;
3. Johns DP, Walters JAE, Walters EH. Diagnosis and early detection of COPD using spirometry. *J Thorac Dis*. 2014;6(11):1557–69.
4. Lu HH, Zeng HH, Chen Y. Early chronic obstructive pulmonary disease: A new perspective. *Chronic Dis Transl Med*. 2021;7(2):79–87.
5. Wu Y, Xia S, Liang Z, Chen R, Qi S. Artificial intelligence in COPD CT images: identification, staging, and quantitation. *Respir Res*. 2024;25(1):319.
6. Purohit S, Dutt N, Saini L, Panwar R, Kumar S. High resolution computed tomography in chronic obstructive pulmonary disease patients: Do not forget radiation hazard. *Lung India*. 2016;33(5):582–3.
7. Sverzellati N, Molinari F, Pirroni T, Bonomo L, Spagnolo P, Zompatori M. New insights on COPD imaging via CT and MRI. *Int J Chron Obstruct Pulmon Dis*. 2007;2(3):301–12.
8. Lu D, Yu H, Chen L, Lin J, Chen S, Huang Y. Differences in the Quantitative HRCT Characteristics of Patients with Asthma, COPD and Asthma–COPD Overlap and Their Relationships with Pulmonary Function. *Int J Chron Obstruct Pulmon Dis*. 2024;Volume 19:1775–89.
9. Gupta PP, Yadav R, Verma M, Agarwal D, Kumar M. Correlation between high-resolution computed tomography features and patients’ characteristics in chronic obstructive pulmonary disease. *Ann Thorac Med*. 2008;3(3):87–93.
10. Torres PPTES, Rabahi MF, Moreira MA do C, Escuissato DL, Meirelles G de SP, Marchiori E. Importance of chest HRCT in the diagnostic evaluation of fibrosing interstitial lung diseases. *J Bras Pneumol publicacao Of da Soc Bras Pneumol e Tisiologia*. 2021;47(3):e20200096.

11. Gershon AS, Warner L, Cascagnette P, Victor JC, To T. Lifetime risk of developing chronic obstructive pulmonary disease: a longitudinal population study. *Lancet* (London, England). 2011;378(9795):991–6.
12. Buist AS, McBurnie MA, Vollmer WM, Gillespie S, Burney P, Mannino DM, et al. International variation in the prevalence of COPD (the BOLD Study): a population-based prevalence study. *Lancet*. 2007;370(9589):741–50.
13. Soriano J. Global, regional, and national deaths, prevalence, disability-adjusted life years, and years lived with disability for chronic obstructive pulmonary disease and asthma, 1990-2015: a systematic analysis for the Global Burden of Disease Study 2015. *Lancet Respir Med*. 2017;5(9):691–706.
14. Janelle V. Chronic obstructive pulmonary disease among adults--United States, 2011. *Morb Mortal Wkly Rep*. 2012 Nov;61(46):938–43.
15. Kochanek KD, Murphy SL, Xu J, Arias E. Mortality in the United States, 2016. *Centers Dis Control Prev*. 2017;293:1–8.
16. Rennard SI, Vestbo J. COPD: the dangerous underestimate of 15%. *Lancet*. 2006;367(9518):1216–9.
17. Murray CJL, Lopez AD. Alternative projections of mortality and disability by cause 1990–2020: Global Burden of Disease Study. *Lancet*. 1997;349(9064):1498–504.
18. Lopez AD, Shibuya K, Rao C, Mathers CD, Hansell AL, Held LS, et al. Chronic obstructive pulmonary disease: current burden and future projections. *Eur Respir J*. 2006;27(2):397–412.
19. Salvi S, Kumar GA, Dhaliwal RS, Paulson K, Agrawal A, Koul PA, et al. The burden of chronic respiratory diseases and their heterogeneity across the states of India: the Global Burden of Disease Study 1990–2016. *Lancet Glob Heal*. 2018;6(12):e1363–74.
20. Agustí A, Celli BR, Criner GJ, Halpin D, Anzueto A, Barnes P, et al. Global Initiative for Chronic Obstructive Lung Disease 2023 Report: GOLD Executive Summary. *Am J Respir Crit Care Med*. 2023;207(7):819–37.
21. Allinson JP, Hardy R, Donaldson GC, Shaheen SO, Kuh D, Wedzicha JA. The Presence of Chronic Mucus Hypersecretion across Adult Life in Relation to Chronic Obstructive Pulmonary Disease Development. *Am J Respir Crit Care Med*. 2016;193(6):662–72.

22. Mejza F, Gnatiuc L, Buist AS, Vollmer WM, Lamprecht B, Obaseki DO, et al. Prevalence and burden of chronic bronchitis symptoms: results from the BOLD study. *Eur Respir J*. 2017;50(5).
23. Elbehairy AF, Raghavan N, Cheng S, Yang L, Webb KA, Neder JA, et al. Physiologic characterization of the chronic bronchitis phenotype in GOLD grade IB COPD. *Chest*. 2015;147(5):1235–45.
24. Regan EA, Lynch DA, Curran-Everett D, Curtis JL, Austin JHM, Grenier PA, et al. Clinical and Radiologic Disease in Smokers With Normal Spirometry. *JAMA Intern Med*. 2015;175(9):1539–49.
25. Rennard SI. COPD: overview of definitions, epidemiology, and factors influencing its development. *Chest*. 1998;113(4):235S-241S.
26. McDonough JE, Yuan R, Suzuki M, Seyednejad N, Elliott WM, Sanchez PG, et al. Small-airway obstruction and emphysema in chronic obstructive pulmonary disease. *N Engl J Med*. 2011;365(17):1567–75.
27. Woodruff PG, Barr RG, Bleecker E, Christenson SA, Couper D, Curtis JL, et al. Clinical Significance of Symptoms in Smokers with Preserved Pulmonary Function. *N Engl J Med*. 2016;374(19):1811–21.
28. Aoshiba K, Nagai A. Differences in airway remodeling between asthma and chronic obstructive pulmonary disease. *Clin Rev Allergy Immunol*. 2004;27(1):35–43.
29. Estépar RSJ, Kinney GL, Black-Shinn JL, Bowler RP, Kindlmann GL, Ross JC, et al. Computed tomographic measures of pulmonary vascular morphology in smokers and their clinical implications. *Am J Respir Crit Care Med*. 2013;188(2):231–9.
30. Barnes PJ, Celli BR. Systemic manifestations and comorbidities of COPD. *Eur Respir J*. 2009;33(5):1165 LP – 1185.
31. Kessler R, Partridge MR, Miravittles M, Cazzola M, Vogelmeier C, Leynaud D, et al. Symptom variability in patients with severe COPD: a pan-European cross-sectional study. *Eur Respir J*. 2011;37(2):264–72.
32. Sin DD, Wu L, Man SFP. The relationship between reduced lung function and cardiovascular mortality: a population-based study and a systematic review of the literature. *Chest*. 2005;127(6):1952–9.

33. Eisner MD, Blanc PD, Yelin EH, Sidney S, Katz PP, Ackerson L, et al. COPD as a systemic disease: impact on physical functional limitations. *Am J Med.* 2008;121(9):789–96.
34. Kjensli A, Falch JA, Ryg M, Blenk T, Armbrecht G, Diep LM, et al. High prevalence of vertebral deformities in COPD patients: relationship to disease severity. *Eur Respir J.* 2009;33(5):1018–24.
35. Badgett RG, Tanaka DJ, Hunt DK, Jelley MJ, Feinberg LE, Steiner JF, et al. Can moderate chronic obstructive pulmonary disease be diagnosed by historical and physical findings alone? *Am J Med.* 1993;94(2):188–96.
36. Lemyze M, Bart F. Hoover sign. *CMAJ.* 2011;183(2):E133.
37. Garcia-Pachon E, Padilla-Navas I. Frequency of Hoover’s sign in stable patients with chronic obstructive pulmonary disease. *Int J Clin Pract.* 2006;60(5):514–7.
38. Quezada WA, Whippo BA, Jellen PA, Leidy NK, Mannino DM, Kim KJ, et al. How Well Does CAPTURE Translate?: An Exploratory Analysis of a COPD Case-Finding Method for Spanish-Speaking Patients. *Chest.* 2017;152(4):761–70.
39. Martinez FJ, Mannino D, Leidy NK, Malley KG, Bacci ED, Barr RG, et al. A New Approach for Identifying Patients with Undiagnosed Chronic Obstructive Pulmonary Disease. *Am J Respir Crit Care Med.* 2017;195(6):748–56.
40. Global strategy for prevention, diagnosis and management of COPD: 2024 report. 2024.
41. Nakano Y, Wong JC, de Jong PA, Buzatu L, Nagao T, Coxson HO, et al. The prediction of small airway dimensions using computed tomography. *Am J Respir Crit Care Med.* 2005;171(2):142–6.
42. Gupta PP, Yadav R, Verma M, Gupta KB, Agarwal D. High-resolution computed tomography features in patients with chronic obstructive pulmonary disease. *Singapore Med J.* 2009;50(2):193.
43. Martinez CH, Chen YH, Westgate PM, Liu LX, Murray S, Curtis JL, et al. Relationship between quantitative CT metrics and health status and BODE in chronic obstructive pulmonary disease. *Thorax.* 2012;67(5):399–406.
44. Shah A, Shah U, Jayalakshmi TK, Mirchandani L, Iyer A, Nair G. COPD phenotypes according to high resolution CT scan findings. *Eur Respir J.* 2014;44(58):P3001.

45. Singh A, Kumar S, Mishra AK, Kumar M, Kant S, Verma SK, et al. Correlation between clinical characteristics, spirometric indices and high resolution computed tomography findings in patients of chronic obstructive pulmonary disease. *Lung India*. 2016;33(1):42–8.
46. Bhaskar R, Singh S, Singh P. Characteristics of COPD phenotypes classified according to the findings of HRCT and spirometric indices and its correlation to clinical characteristics. *Afr Health Sci*. 2018;18(1):90–101.
47. Rao P, Talatam A, Chakradhar B, Bhargavi K, Bhagyaraj A. High resolution computed tomography in chronic obstructive pulmonary disease. *Int J Adv Med*. 2018;5(5):1222–6.
48. Bodduluri S, Reinhardt JM, Hoffman EA, Newell Jr JD, Bhatt SP. Recent advances in computed tomography imaging in chronic obstructive pulmonary disease. *Ann Am Thorac Soc*. 2018;15(3):281–9.
49. Bhatt SP, Washko GR, Hoffman EA, Newell Jr JD, Bodduluri S, Diaz AA, et al. Imaging advances in chronic obstructive pulmonary disease. Insights from the genetic epidemiology of chronic obstructive pulmonary disease (COPDGene) study. *Am J Respir Crit Care Med*. 2019;199(3):286–301.
50. Vimala LR, Gibikote S, Irodi A, Rajan M, Christopher DJ. Correlation of quantitative and qualitative parameters of high-resolution computed tomography with pulmonary function test for diagnosing and assessing the severity of obstructive pulmonary disease. *Polish J Radiol*. 2019;84:381–8.
51. Soleeva NB, Sayfiev FD, Turdumatov JA, Mansurov DN. Computed tomography capabilities in the diagnosis of chronic obstructive pulmonary disease. *Вестник магистратуры*. 2022;(2-2 (125)):15–8.
52. Zhu D, Qiao C, Dai H, Hu Y, Xi Q. Diagnostic efficacy of visual subtypes and low attenuation area based on HRCT in the diagnosis of COPD. *BMC Pulm Med*. 2022;22(1):81.
53. Park J, Kim EK, Lee SH, Kim MA, Kim JH, Lee SM, et al. Phenotyping Copd patients with emphysema distribution using quantitative Ct measurement; more severe airway involvement in lower dominant emphysema. *Int J Chron Obstruct Pulmon Dis*. 2022;2013–25.

54. Rodrigues Sousa S, Nunes Caldeira J, Rodrigues C. COPD phenotypes by computed tomography and ventilatory response to exercise. *Pulmonology*. 2024;30(3):222–9. Kaufman A, Pruzan A, Hsu C, Ramachandran S, Jacobi A, Patel I, Schwocho L, Mercuri M, Fayad Z, Mani V. Reproducibility of thrombus volume quantification in multicenter computed tomography pulmonary angiography studies. *World J Radiol*. 2018;10:124-134. doi:10.4329/wjr.v10.i10.124.

ANNEXURE I
KAHERs JNMC
BELAGAVI
INFORMED CONSENT FORM

“Role of High Resolution Computed Tomography thorax in assessment of various imaging patterns in chronic obstructive pulmonary disease-a one year cross sectional study in a tertiary care hospital”

Principal Investigator(PI): BS0122013

Introduction: High Resolution computed tomography of thorax is capable of imaging the lung with excellent spatial resolution which can readily demonstrate the normal and abnormal lung interstitium and morphologic characteristics of both localised and diffuse parenchymal abnormalities. CT has advantage of allowing direct measurement of airway dimensions , including those associated with luminal narrowing and wall thickening, and can also be used to estimate air trapping . It provides a non invasive method for the detection of potentially reversible airway abnormalities, and permits a regional assessment of airways.

Explanation of procedure: The purpose of the study will be explained and written informed consent shall be obtained from all the participants. The subjects will be selected based on inclusion and exclusion criteria. Study will be conducted over a period of one year. once the patients signs informed consent , history and examination will be done. As part of the study , you will subjected to High Resolution Computed Tomography(HRCT) scan of chest. Please wear loose fitting and comfortable clothing to your scan. remove any metal objects, including jewelry, eye glasses, and mobile phones prior to the scan. The technologists will ask you a few questions of the regarding your medical history and will give a detailed explanation about the steps involved in the scan. You will be asked to lie flat on your back on CT table with arms over your head . The CT table will then slide into the gantry. The technologist will convey further instructions in your desired language over the intercom. You will be asked to lie very still and hold breath for a few seconds. The entire scan will be completed within five minutes.

Withdrawal from participation in the study: Participation in this study is voluntary. You will be free to decide whether to participate in this study or continue participation once enrolled. In case you decide to withdraw your participation, you are free to do so. However, please convey the decision to the principal investigator.

Possible risks from participating in the study: There are no risks involved in participating in this study as the radiation exposure in HRCT Thorax is low. You need to inform if you are a pregnant or suspect that you may be a pregnant.

Privacy and confidentiality: The information collected from you will be coded, to prevent any person to identify you. Your identity will never be revealed. The data collected from you will be kept confidential and only processed or aggregated data will be used for publication.

Financial incentives: You will not receive any payment for participating in this study.

Authorization for publication of aggregated data: Results obtained after processing of the aggregated data will be published for scientific purpose and or presented to scientific groups. However, your identity will never be revealed.

Questions: In case of any questions with regard to this study, you are free to contact:

REG NO. BS0122013

Post-Graduate,
Department of Radio-Diagnosis.
J.N. Medical College,
KAHER, Belagavi- 590010
Karnataka

Legal rights: By signing this consent form, we are not waiving any of your legal rights

CONSENT STATEMENT

I am making a voluntary decision to participate in the study “Role of High Resolution Computed Tomography thorax in assessment of various imaging patterns in chronic obstructive pulmonary disease-a one year cross sectional study in a tertiary care hospital”. My signature below indicates that I have decided to participate and I have read the information provided above or the information provided above has been read to me in the language that I understand best. I was given the opportunity to ask questions and that they have been answered to my satisfaction.

Name of the participant:

Signature or left thumb impression of the participant:

Name of the witness:

Signature or left thumb impression of the witness:

Name of the investigator:

Signature of the investigator:

ANNEXURE II

PROFORMA

TITLE: Role of High Resolution Computed Tomography thorax in assessment of various imaging patterns in chronic obstructive pulmonary disease-a one year cross sectional study in a tertiary care hospital

NAME:

AGE:

SEX:

OCCUPATION:

IP/OP No:

ADDRESS:

Ph.No:

DATE:

Ref Dr:

CLINICAL COMPLAINTS:

PAST HISTORY:

CLINICAL DIAGNOSIS:

HRCT THORAX FINDINGS:

HRCT FEATURES	FINDINGS
Saber -sheath trachea	
Thoracic cage ratio at carina	
Thoracic cage ratio at 5 cm below carina	
Sterno -aortic distance > 4 cm	
Thoracic cross-sectional area/height ²	
Vascular attenuation	
Vascular distortion	
Mosaic attenuation pattern	
Directly visible small airways	

HRCT REPORT:

ANNEXURE III: IMAGES

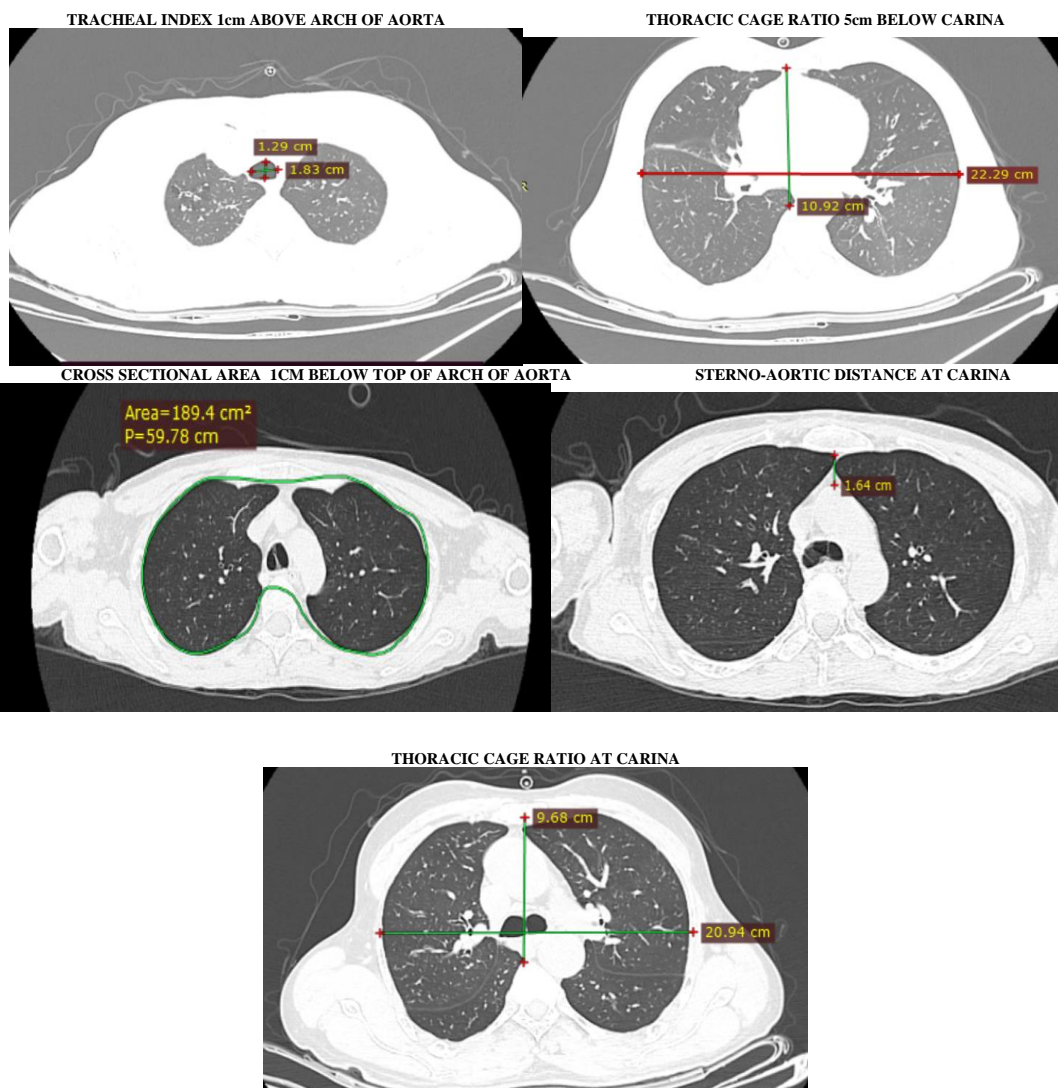
128-slice CT scanner (General Electronics (GE) Revolution, single-tube machine) used for the study



IMAGES OF CASES

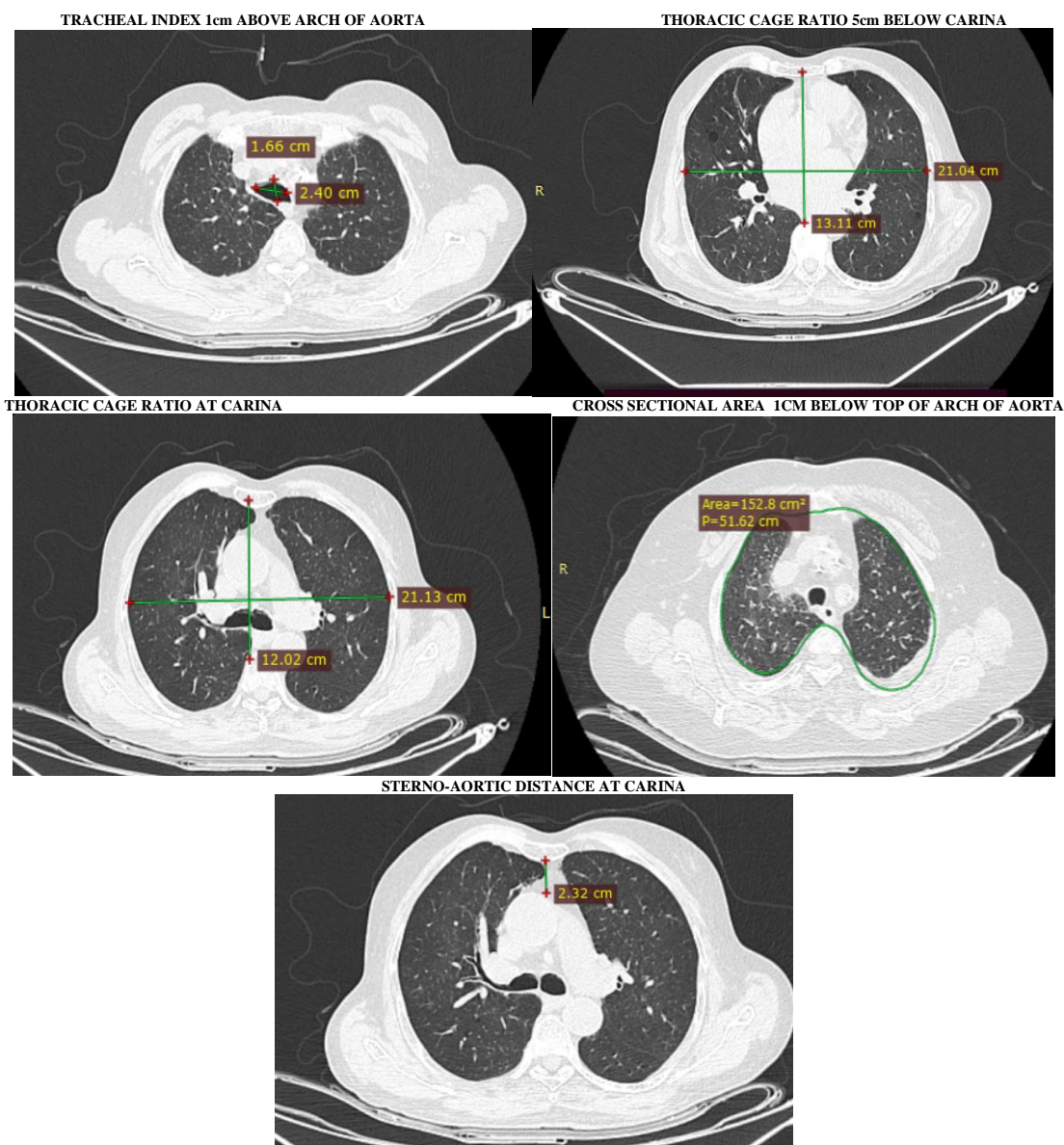
CASE 1: A 56 year old male with history of chronic cough and dyspnea for past 2 years on and off with history of smoking and spirometry GOLD grade 1

HRCT Thorax in axial section lung window showing few areas of centrilobular emphysematous changes sterno-aortic distance of 1.6 cm, tracheal index of 1.3, thoracic ratio 0.4 at carina and 0.5 – 5cm below carina with cross sectional area / height sq (1.5 in meters) is 74.



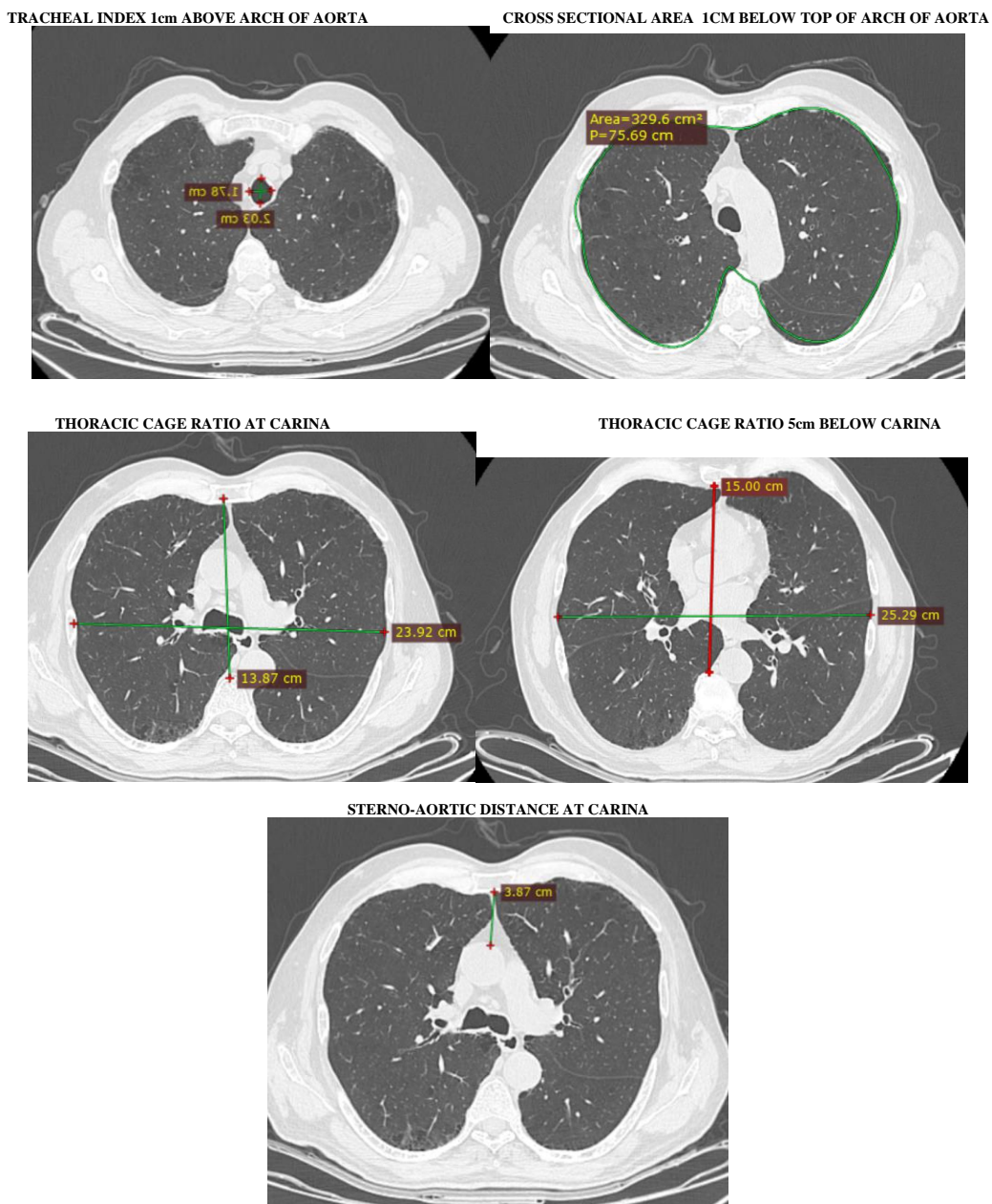
CASE 2 : A 73 Year old male came with complaints of cough and dyspnea for past 4 months, height of 1.6 meters and spirometry values as GOLD grade 2.

HRCT thorax in axial section in the lung window showing, sterno-aortic distance of 2.3 cm at the carina with tracheal index of 1.5 - 1cm above the arch of aorta , thoracic ratio 0.5 at carina and 0.6 - 5cm below the carina and cross sectional / height² is 60.8.



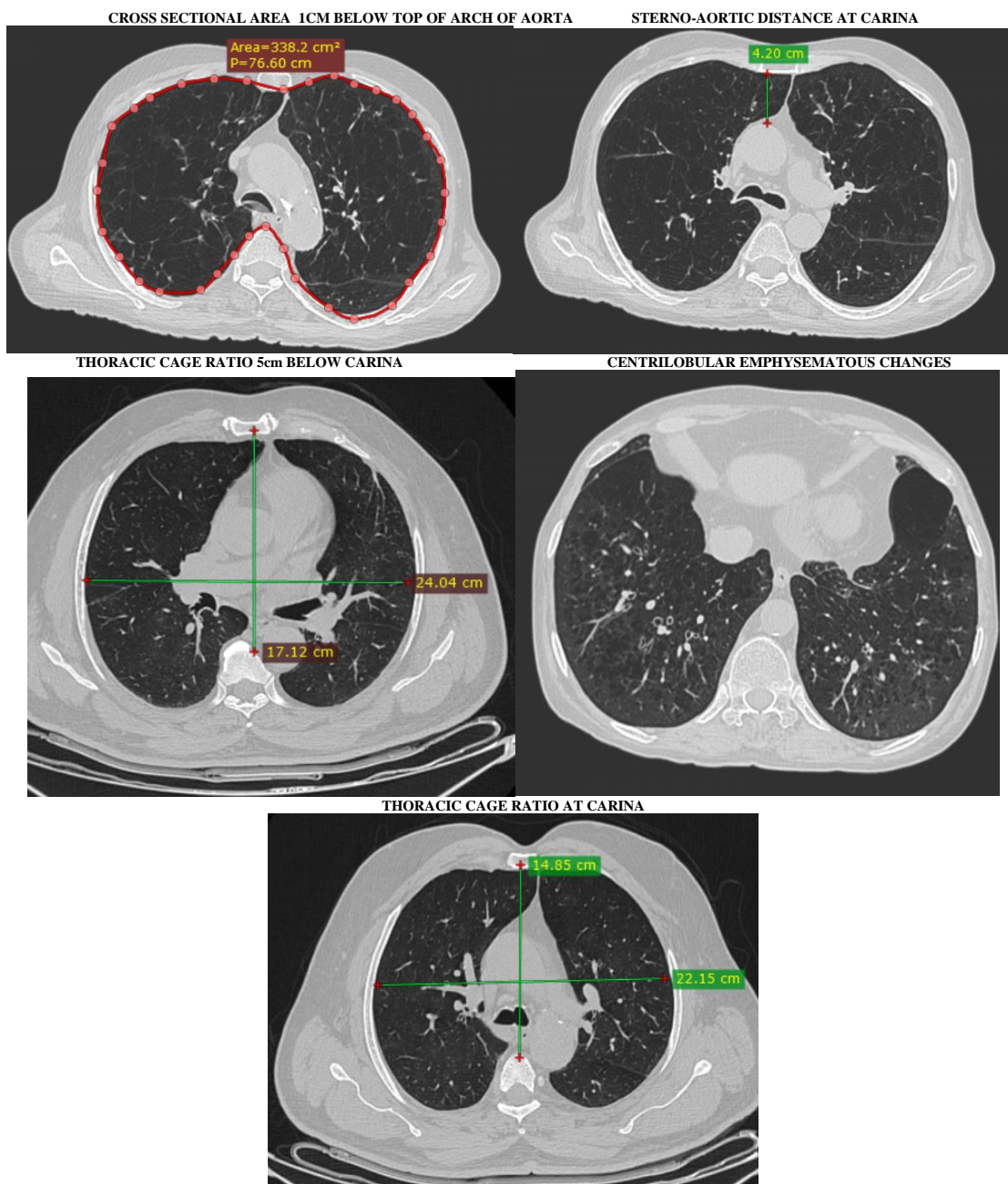
CASE 3 : A 78 year old male came with complaints of cough and dyspnea with history of smoking and on spirometry values gold grade 3

HRCT thorax axial section lung window centrilobular and paraseptal emphysematous changes noted diffusely and vascular attenuation with tracheal index of 0.8 , sterno aortic distance at carina measures 3.8 cm and thoracic ratio at carina measures 0.58 and 0.6 – 5cm below carina with thoracic cross sectional area / height sq (1.6 in meters) measures 120.



CASE 4 : A 69 year old male came with complaints of chronic cough and dyspnea on and off with history of smoking , height of 1.5 meters and spirometry GOLD grade 4.

HRCT thorax lung window in the axial section showing diffuse areas of vascular attenuation & distortion, directly visible small airways, mosaic attenuation pattern with centrilobular emphysematous changes and a sterno-aortic distance of 4.2 cm, thoracic ratio at carina measures 0.63 and 0.7 – 5cm below carina cross sectional area/ height² of 150



ANNEXURE - IV

KEY TO MASTER CHART

MALE	M
FEMALE	F
HYPERTENSION	HTN
ISHEMIC HEART DISEASE	IHD
NOT ASSOCIATED WITH DISEASE	NAD
WITHIN NORMAL LIMITS	WNL
NORMAL VESICULAR BREATH SOUNDS	NVBS
PRESENT	P
ABSENT	A

ANNEXURE - V

MASTER CHART

S. No	Age	Occupation	comorbidities	Family History	Smoking History	physical examination	HEIGHT	BMI	RESPIRATORY SYSTEM	GOLD GRADE	FEV1	FVC	FEV1/FVC	FEF25-75%	PEFR	Sex
1	78	Private employe	HTN,IHD	Nad	P	WNL	1.56	19.60	Crepts	2	62.82	96.97	0.65	66	49	M
2	68	Farmer	T2DM,HTN,IHD	Nad	P	BARREL CHEST	1.62	32.05	Nvbs	2	62	71	0.7	49	52	M
3	32	Private employe	NIL	Nad	P	WNL	1.66	26.08	Nvbs	2	69.52	102.24	0.68	56	59	M
4	57	House wife	A	Nad	A	WHEEZE	1.62	22.32	Nvbs	2	52.8	75.43	0.5	28	32	F
5	74	Shopkeeper	HTN, T2DM	Nad	P	WNL	1.54	25.28	Nvbs	2	73.04	104.34	0.7	48	39	M
6	78	Private employe	HTN, T2DM	Nad	P	WNL	1.63	23.73	Nvbs	2	70.4	100.57	0.7	42	66	M
7	43	Private employe	A	Nad	A	WNL	1.54	31.11	Nvbs	2	52.8	75.43	0.7	36	40	F
8	76	Farmer	T2DM,HTN,IHD	Nad	P	WNL	1.52	19.23	Nvbs	2	63.33	107.92	0.59	50	66	M
9	77	Carpenter	HTN, ASTHMA	Nad	P	WNL	1.63	19.57	Nvbs	2	65.12	93.03	0.7	50	40	M
10	59	Home maker	A	Nad	A	WNL	1.69	29.64	Nvbs	2	62	71	0.7	49	52	F
11	78	Labourer	HTN	Nad	P	WNL	1.72	30.47	Nvbs	2	77.44	123.2	0.63	50	68	M
12	79	Farmer	T2DM	Nad	P	WNL	1.49	19.57	Nvbs	2	65.12	93.03	0.7	55	62	M
13	77	Farmer	HTN	Nad	A	WNL	1.63	22.50	Nvbs	2	65.1	92	0.7	62	70	F
14	78	Farmer	HTN, DM, IHD	Nad	P	WNL	1.52	21.08	Nvbs	2	52.8	75.43	0.5	28	32	M
15	73	Farmer	A	Nad	P	WNL	1.66	24.22	Nvbs	1	81.48	115.85	0.7	58	66	M
16	60	Kooli	A	Nad	P	WNL	1.62	22.94	Nvbs	3	45	59	0.69	34	28	M
17	73	House wife	HTN,T2DM	Nad	A	WNL	1.55	24.65	Nvbs	2	55.43	65	0.67	58	66	F
18	72	House wife	HTN,DM,IHD	Nad	A	WNL	1.59	20.82	Nvbs	2	70.4	100.57	0.7	20	22	F
19	78	Trader	HTN, DM	Nad	P	WNL	1.63	19.84	Rhonchi	3	42.24	60.34	0.7	52	42	M
20	44	Bank employe	T2DM,HTN	Nad	P	WNL	1.54	20.76	Nvbs	3	45	59	0.69	34	28	M
21	69	Farmer	HTN	Nad	P	WNL	1.63	19.49	Nvbs	4	29.04	41.49	0.7	15	6	M
22	70	Farmer	DM	Copd	P	BARREL SHAPED CHEST	1.54	16.23	Nvbs	2	65.12	93.03	0.7	52	40	M
23	36	Private employe	A	Nad	A	WNL	1.52	19.63	Nvbs	2	63.36	90.5	0.7	66	52	M
24	66	Sugar factory	T2DM,HTN,IHD	Nad	P	WNL	1.63	30.47	Nvbs	2	50.16	84.48	0.59	32	72	M
25	65	Vendor	A	Nad	A	WNL	1.69	27.12	Nvbs	2	54.56	77.94	0.7	52	43	M
26	70	Farmer	HTN, DM	Nad	P	WNL	1.72	30.47	Nvbs	2	65.12	93.03	0.7	58	73	M
27	53	Farmer	HTN	Nad	A	WNL	1.49	22.43	Nvbs	2	52.8	75.43	0.7	36	40	F
28	55	Cook	A	Nad	P	WNL	1.63	24.22	Nvbs	2	70.4	100.57	0.7	42	66	M
29	70	Farmer	T2DM,HTN	Nad	P	WNL	1.61	22.86	Nvbs	2	52.8	89.6	0.59	39	52	M

Master Chart

30	53	Farmer	HTN	Nad	A	WNL	1.72	19.07	Nvbs	2	52.8	75.43	0.7	36	40	F
31	71	Farmer	HTN	Nad	P	WNL	1.54	22.04	Nvbs	3	46	66	0.69	28	38	M
32	78	Farmer	HTN, DM, IHD	Nad	P	WNL	1.63	19.88	Nvbs	3	44	70.4	0.63	33	40	M
33	73	Farmer	HTN, DM, IHD	Nad	P	BARREL CHEST	1.54	20.83	Nvbs	2	52.8	89.6	0.59	39	52	M
34	64	Land loard	T2DM	Nad	A	WNL	1.52	21.64	Nvbs	3	45	59	0.69	34	28	M
35	59	Farmer	T2DM,HT N,IHD	Nad	P	WNL	1.63	25.82	Scattered crepts	2	70	78	0.7	41	48	M
36	66	Shop keeper	HTN	Nad	P	WNL	1.69	33.73	Nvbs	3	45.76	65.37	0.7	24	28	M
37	60	Farmer	T2DM	Nad	P	WNL	1.72	22.50	Nvbs	2	66.23	97.9	0.68	46	60	M
38	63	Farmer	HTN,T2D M,IHD	Nad	P	WNL	1.49	23.60	Nvbs with scattered crepts	3	45.76	65.37	0.7	24	28	M
39	62	Farmer	T2DM, HTN, IHD	Nad	P	WNL	1.63	19.23	Nvbs	2	54.56	77.94	0.7	54	47	M
40	79	Shopkeeper	T2DM,HT N	Nad	P	WNL	1.58	17.06	B/l crepts	2	66.23	97.9	0.68	46	60	M
41	69	Farmer	T2DM	Nad	P	WNL	1.69	20.32	Nvbs	2	65.74	99.98	0.66	60	82	M
42	31	Bank employe e	A	Nad	P	WNL	1.66	19.23	Nvbs	2	54.56	77.94	0.7	52	43	M
43	54	House wife	A	Nad	A	WNL	1.54	26.99	Nvbs	2	58.08	100.8	0.58	72	40	F
44	75	Labourer	HTN	Nad	P	WNL	1.63	24.22	Nvbs	2	65.12	95.76	0.68	31	48	M
45	68	House wife	HTN	Nad	A	WNL	1.54	23.60	Nvbs	3	46	66	0.69	28	38	F
46	52	House wife	HTN, IHD	Nad	A	WNL	1.52	17.71	Bilateral basal crepts	3	49.28	70.4	0.7	25	27	F
47	78	Land loard	A	Nad	P	WNL	1.63	22.04	Nvbs	2	56.32	82.82	0.68	47	88	M
48	71	Farmer	A	Nad	P	WNL	1.69	17.72	Nvbs	2	68	92	0.7	53	27	M
49	58	Labourer	T2DM, HTH	Cop d	P	WNL	1.72	30.47	Nvbs	2	53.65	53	0.67	62	70	M
50	65	House wife	T2DM,HT N,IHD	Nad	A	WNL	1.49	28.04	Nvbs	2	66.88	95.54	0.7	38	52	F
51	68	Farmer	A	Asth ma	P	WNL	1.63	24.38	Nvbs	2	54.56	77.94	0.7	52	43	M
52	56	Farmer	A	Nad	P	WNL	1.54	18.36	Nvbs	3	40	66.7	0.66	32	40	M
53	56	Industrial worker	HTN, DM	Nad	P	WNL	1.52	19.88	Nvbs	2	65.12	93.03	1	66	50	M
54	35	Shopkeeper	A	Nad	P	WNL	1.63	23.73	Nvbs	1	81.57	98	0.7	55	62	M
55	70	Farmer	HTN	Nad	P	WNL	1.69	33.73	Nvbs	2	62.82	96.97	0.65	66	49	M
56	68	House wife	HTN	Nad	A	WNL	1.72	25.51	Nvbs	3	46	66	0.69	28	38	F
57	77	Farmer	A	Nad	P	WNL	1.49	23.44	Nvbs	2	65.1	92	0.7	62	70	M
58	77	Farmer	HTN	Nad	P	WNL	1.63	22.27	Nvbs	2	65.74	99.98	0.66	60	82	M
59	43	Labourer	T2DM	Nad	P	WNL	1.54	24.34	Nvbs	2	66.23	97.9	0.68	46	60	M
60	72	Farmer	HTN	Nad	P	WNL	1.63	19.84	Nvbs	2	65.25	98.24	0.66	61	68	M
61	67	Farmer	A	Nad	P	WNL	1.54	18.55	Nvbs	2	60.72	95.2	0.64	38	30	M
62	78	Vender	HTN,DM,I HD	Nad	P	WNL	1.52	27.28	Vbs	3	39.6	56.57	0.7	22	27	M
63	55	Labourer	A	Nad	P	WNL	1.63	24.46	Nvbs	2	52.8	75.43	0.5	28	32	M
64	67	Labourer	T2DM,HT N	Nad	P	WNL	1.69	25.71	Nvbs	2	52.8	89.6	0.59	39	52	M
65	68	Farmer	A	Nad	P	WNL	1.72	26.37	Nvbs	2	65.12	93.03	0.7	40	59	M
66	56	Farmer	A	Nad	P	WNL	1.49	18.36	Nvbs	2	51.04	84.48	0.6	62	66	M
67	72	House wife	HTN	Nad	A	WNL	1.63	25.71	Nvbs	2	58	74	0.6	24	28	F
. No	Emphysematous Changes(Centrilobular/Paraseptal/Panac inar)				Saber Sheat Trachea (Thoracic Index)			Thoraci c Cage Ratio At Carina >0.75	Thoracic Cage Ratio 5cm Below Carina >0.75	Ster no Aorti c Dista nce In Cm	Thoraci c Cross Section al Area/ Height Sq (Cm/Ms q)	Vascula r Attenuat ion	Vascul ar Distorti on	Moasa ic Attenu ation Patter n	Dire ctly Visi ble Sma ll Airw ays	
1	CENTRILOBULAR & PARASEPTAL				A(0.9)			0.44	0.47	2.3	89	P	A	A	P	

Master Chart

2	CENTRIOBULAR & PARASEPTAL	A(0.7)	0.7	0.62	2.8	78	P	A	A	P
3	CENTRIOBULAR	A(0.7)	0.38	0.45	2.3	57	A	A	A	P
4	A	A(1.2)	0.49	0.54	1.5	44	A	A	A	P
5	CENTRIOBULAR	A (1.3)	0.52	0.53	4.2	91	P	A	P	P
6	CENTRIOBULAR & PARASEPTAL	A (1.3)	2	2.1	3.4	52	A	A	A	A
7	A	A (0.8)	2.2	1.9	2.2	98	A	A	A	A
8	CENTRIOBULAR	A (0.8)	0.3	0.4	2.3	56	P	A	A	A
9	CENTRIOBULAR & PARASEPTAL	A (0.8)	0.6	0.7	2.5	78	P	A	A	P
10	A	A(0.7)	0.39	0.45	2.8	88	A	P	A	A
11	CENTRIOBULAR & PARASEPTAL	A (0.8)	0.5	0.5	2.9	66	P	A	A	A
12	CENTRIOBULAR	A (0.9)	0.4	0.4	1.9	55	A	A	A	A
13	CENTRIOBULAR	A (1.0)	0.35	0.39	1.1	69	A	A	A	A
14	PARASEPTAL	A (1.3)	0.36	0.47	1.6	80	A	A	A	A
15	CENTRIOBULAR	A (0.9)	0.5	0.49	3.4	57	A	A	A	A
16	CENTRIOBULAR	A (1.0)	0.39	0.4	1.1	54	A	A	A	A
17	CENTRIOBULAR	A (1.0)	0.35	0.38	1.4	45	A	A	P	A
18	PARASEPTAL	A (1.3)	0.5	0.55	1	60	A	P	P	A
19	CENTRIOBULAR	A (0.8)	0.48	0.5	1.1	50.8	P	A	P	P
20	PARASEPTAL	A (0.8)	0.43	0.5	2.3	94	P	A	P	A
21	CENTRIOBULAR & PARASEPTAL	P (0.6)	0.5	0.6	3.5	120	P	P	A	A
22	CENTRIOBULAR	A (1.0)	0.5	0.4	1.8	66	P	A	A	A
23	A	A(1.2)	0.6	0.7	3.4	63	A	A	P	A
24	PARASEPTAL	A (0.7)	0.37	0.45	2	75	P	A	A	A
25	CENTRIOBULAR & PARASEPTAL	A (0.9)	0.38	0.4	1.9	102	P	P	A	P
26	CENTRIOBULAR	A (1.1)	0.5	0.54	2.6	60.9	P	A	P	P
27	A	A (0.9)	0.35	0.43	0.8	99	P	A	P	P
28	A	A (1.0)	0.36	0.38	0.8	68.6	A	A	P	A
29	CENTRIOBULAR & PARASEPTAL	A (0.8)	0.57	0.59	4.06	128	P	A	P	P
30	PANACINAR	A(1.6)	0.4	0.5	2.2	244	P	P	P	P
31	CENTRIOBULAR & PARASEPTAL	A (1.0)	0.4	0.5	1.7	77.1	P	A	P	A
32	CENTRIOBULAR & PARASEPTAL	A (0.8)	0.39	0.5	0.9	57.9	P	P	P	P
33	A	A (1.3)	0.4	0.48	1.1	76.5	P	P	P	A
34	CENTRIOBULAR & PARASEPTAL	A(1.2)	0.5	0.6	3	35	P	A	P	A
35	PARASEPTAL	A (1.0)	0.46	0.47	3	95	P	P	P	P
36	A	A (0.8)	0.58	0.66	5.2	38	P	A	P	P
37	CENTRIOBULAR & PARASEPTAL	A (1.05)	0.42	0.55	2	158	A	A	P	P
38	A	A(1.2)	0.51	0.52	2	69	P	A	P	A
39	A	A(0.7)	0.45	0.49	4.1	64.9	A	A	P	A
40	CENTRIOBULAR	A (0.8)	0.44	0.52	0.7	75.7	P	P	A	A
41	CENTRIOBULAR	A (0.8)	0.54	0.61	4.1	103	P	P	P	A
42	A	A (0.9)	0.28	0.38	1.9	54	P	A	A	P
43	A	A (1.0)	0.36	0.43	0.6	70.4	A	A	P	A
44	A	A(1.1)	0.4	0.49	1.1	113	P	A	P	A

Master Chart

45	A	A (1.0)	0.5	0.8	2.3	46	P	P	P	P
46	A	A (1.0)	0.5	0.5	2.3	18	A	A	A	A
47	A	A(0.7)	0.59	0.65	4.03	58	P	A	A	A
48	A	A (0.9)	0.5	0.52	2.4	124	A	A	A	A
49	A	A (0.8)	0.49	0.47	3	122	A	A	A	P
50	PARASEPTAL	A (0.9)	0.39	0.45	2.5	105.4	A	A	A	A
51	CENTRILOBULAR & PARASEPTAL	A(1.1)	0.52	0.5	2.9	110	A	A	P	A
52	CENTRILOBULAR	A (1.0)	0.5	0.58	2.9	137	P	A	A	A
53	CENTRILOBULAR	A (1.0)	0.46	0.53	1.8	124	P	P	P	P
54	A	A (1.0)	0.39	0.53	2.9	86	P	P	P	P
55	A	A (1.0)	0.5	0.5	1.9	163	A	A	A	A
56	A	A(1.1)	0.36	0.39	1.1	35	P	P	A	A
57	A	A(1.2)	0.45	0.45	1.2	88	A	A	A	A
58	A	A(1.4)	0.56	0.62	2.3	58	P	A	A	P
59	A	A(1.1)	0.53	0.51	2.6	77	P	A	P	A
60	A	A(1.2)	0.4	0.4	0.8	40	A	A	A	A
61	A	A(0.7)	0.4	0.5	2.2	158	A	A	A	P
62	A	P (0.5)	0.8	0.8	2.6	160	A	A	A	A
63	A	A(1.0)	0.4	0.56	0.56	206	A	A	A	A
64	A	A(1.3)	0.48	0.52	2.6	81	A	A	A	A
65	A	A(0.7)	0.6	0.58	3	130	A	A	A	A
66	A	A(1.1)	0.48	0.5	3.4	76	A	A	A	A
67	A	A(1.2)	0.4	0.5	1.4	70	A	A	A	A